

MEMO 3-17-59E

IN-02
394 527

NASA

MEMORANDUM

ANALYSIS AND EVALUATION OF SUPERSONIC
UNDERWING HEAT ADDITION

By Roger W. Luidens and Richard J. Flaherty

Lewis Research Center
Cleveland, Ohio

NATIONAL AERONAUTICS AND
SPACE ADMINISTRATION
WASHINGTON
April 1959

NATIONAL AERONAUTICS AND SPACE ADMINISTRATION

MEMORANDUM 3-17-59E

ANALYSIS AND EVALUATION OF SUPERSONIC UNDERWING HEAT ADDITION

By Roger W. Luidens and Richard J. Flaherty

SUMMARY

The linearized theory for heat addition under a wing has been developed to optimize wing geometry, heat addition, and angle of attack. The optimum wing has all of the thickness on the underside of the airfoil, with maximum-thickness point well downstream, has a moderate thickness ratio, and operates at an optimum angle of attack. The heat addition is confined between the fore Mach waves from under the trailing surface of the wing. By linearized theory, a wing at optimum angle of attack may have a range efficiency about twice that of a wing at zero angle of attack.

More rigorous calculations using the method of characteristics for particular flow models were made for heating under a flat-plate wing and for several wings with thickness, both with heat additions concentrated near the wing. The more rigorous calculations yield in practical cases efficiencies about half those estimated by linear theory. An analysis indicates that distributing the heat addition between the fore waves from the undertrailing portion of the wing is a way of improving the performance, and further calculations appear desirable.

A comparison of the conventional ramjet plus wing with underwing heat addition when the heat addition is concentrated near the wing shows the ramjet to be superior on a range basis up to Mach number of about 8. The heat distribution under the wing and the assumed ramjet and airframe performance may have a marked effect on this conclusion. Underwing heat addition can be useful in providing high-altitude maneuver capability at high flight Mach numbers for an airplane powered by conventional ramjets during cruise.

INTRODUCTION

This report presents an analysis and evaluation of supersonic underwing heat addition. The linear theory is used to optimize wing profile angles, angle of attack, and heat addition. A series of more rigorous calculations using the method of characteristics is made for comparison

with the linear theory. The advantage of the linearized theory is the ease with which a wide variety of wing geometries, heat addition, and airplane application can be considered. The disadvantage of the linear theory is that it can deviate widely from the more rigorous calculations in the range of heat additions of practical interest.

A comparison is made between underwing heat addition and the conventional wing-plus-ramjet configuration. The following cases are considered: (1) All the propulsion is provided by underwing heat addition, (2) only a fraction of the thrust is provided by underwing addition, with remaining thrust developed by a ramjet, and (3) ramjet propulsion is used for cruise and underwing heat addition for maneuver. The effect of underwing heat addition on airplane weights and hence range is also discussed.

Some of the initial work in the field of supersonic heat addition is given in references 1 and 2. The method presented, although accurate, is time-consuming. References 3 and 4 develop the zero-angle-of-attack linear theory by approaches different from that of this report but arrive at the same result. Reference 5 discusses optimum wing shapes as determined by linearized theory and arrives at essentially the same conclusions from the linear theory as this report, again from a different approach. References 6 to 9 present results of some experiments with burning of a fuel injected adjacent to a flat plate at supersonic speeds. No comparisons are made between experiment and theory. However, the experimental results do show a substantial pressure rise due to heat addition. Distinctive contributions of this report are the comparison of the linear theory with some nonlinearized calculations and a study of the applications of underwing heat addition with respect to the over-all airplane mission. In appendix C, the effect of supersonic underwing heat addition is derived from potential-flow equations by Stephen H. Maslen.

ANALYSIS AND DISCUSSION

The analysis is developed from the point of view of using underwing burning for cruise propulsion or for maneuvering at supersonic speeds, or both. The burning is assumed to take place outside the boundary layer in the supersonic stream. No consideration is given to the problem of how the actual heat addition is accomplished. In general, the details of the analysis are given in appendixes, and the pertinent results are discussed in the body of the report. The report proceeds in the following order: First, performance parameters are discussed; second, these parameters are evaluated by linear theory and by more rigorous calculation; and finally, a performance comparison is made between underwing heat addition and the conventional wing plus ramjet.

Performance Parameters

It is convenient to evaluate underwing burning in terms of a specific lift parameter defined as the lift per Btu per second:

$$\frac{L}{Q} = \frac{L}{hw_f} \quad (1)$$

(The symbols used in this report are defined in appendix A.) This is equivalent to the following terms for the conventional wing plus ramjet:

$$\frac{L}{Q} = \frac{L}{D} \frac{I}{h} \quad (2)$$

The specific lift parameter is related to range through the conventional Breguet range equation as follows:

$$R = \left(\frac{L}{Q} \right) \frac{hV}{1 - \left(\frac{V}{V_s} \right)^2} \ln \left(\frac{1}{1 - \frac{W_f}{W_G}} \right) \quad (3)$$

The range equation applies when thrust is equal to drag and lift is equal to weight. The wing lift coefficient C_L is also of interest, since it determines the wing size and hence its weight, which enters the range equation through the log term.

The parameters important to maneuverability may be determined by considering a turn. The weight of fuel consumed in a turn without loss of speed or altitude is related to the gross weight at the beginning of the turn and to the specific lift by the following equation:

$$\frac{W_f}{W_G} = \frac{e^\zeta - 1}{e^\zeta} \quad (4)$$

where

$$\zeta = \frac{2\pi V n}{g \sqrt{n^2 - 1}} \frac{\Omega}{360^\circ} \frac{1}{h L / Q} \quad (5)$$

The term n is the number of g's normal acceleration in the maneuver and can be expressed as the ratio of the maneuver to cruise lift coefficients,

$$n = \frac{C_{L,n}}{C_{L,c}}$$

By linearized theory, assuming a symmetrical drag polar and cruise at maximum lift-drag ratio,

$$C_{L,c} = \frac{2}{\sqrt{M^2 - 1} (L/D)_{max}}$$

The maneuver lift coefficient $C_{L,n}$ can be the lift coefficient with underwing heat addition. For maximum range and minimum fuel consumed in a maneuver, a high value of L/Q and a high C_L are desirable.

Linearized Solutions

All the linearized solutions of this report are derived for a double-wedge airfoil with the top surface flat. The selection of this profile can be justified on the basis of simplicity for analytical purposes and good performance.

Zero angle of attack. - The analysis of the underwing-heat-addition problem is given in appendix B for the general wing and flow geometry shown in figure 1 for $\alpha = 0$. The analysis assumes two-dimensional flow and makes the usual supersonic linearized flow approximations. From this analysis the specific lift is given by equation (B25) as

$$\left(\frac{L}{Q}\right)_{l,a=0} = \frac{(r - 1)J}{a} \cdot \frac{M}{\sqrt{M^2 - 1}} \quad (6a)$$

where the subscript $l,a=0$ designates linearized theory at zero angle of attack. This result is used as a reference value in the angle-of-attack discussion. The parameter defining the wing lift coefficient for underwing heat addition at zero angle of attack is (eq. (B32))

$$\left(\frac{C_L}{\Delta T}\right)_{l,a=0} = \frac{2 \left(1 + \frac{r - 1}{2} M^2\right)}{M^2 - 1} \quad (6b)$$

where the lift coefficient is based on the wing area affected by the heat addition. The temperature rise across the heat addition ΔT as used here and in subsequent parts of the report, except where otherwise noted, applies to the stream tube of air A_0 and the heat-addition zone shown in figure 1.

Equations (6a) and (6b) are independent of wing profile, as demonstrated by the developments in appendix B leading to these results; hence, they also apply to a flat plate. In addition, although equations (6a)

and (6b) have been designated for zero angle of attack where the lift due to burning is the total lift, the lift increment due to burning is actually independent of angle of attack (eq. (D1)). The incremental specific lift is also independent of the quantity of the heat addition. Appendix C shows that the incremental specific lift is independent of the place where the heat addition occurs as long as it is within the forward Mach lines from the leading and trailing edge of the wing, labeled a and c in figure 1. The specific lift at zero angle of attack or the incremental specific lift depends only on Mach number, γ , and the speed of sound. These results (eqs. (6a) and (6b)) are implicit in the developments of references 3 and 4, which use other approaches to the problem.

Burning also affects the drag of the wing. In order for the specific lift to be used in the range equation, the thrust must equal the drag. The pressure increment due to heat addition is always positive (eqs. (B5) and (C5)). Hence, if the burning influences an upstream-facing region on the wing, there is an increase in drag (eq. (C4)), while for a surface facing downstream there is a drag reduction or a thrust. The most favorable region for heat addition is thus bounded by the fore Mach lines from the downstream-facing areas, labeled b and c, or region II, in figure 1.

By the appropriate heat addition in region II the thrust on the downstream-facing area can be made equal to the pressure drag that exists on the upstream-facing area and the friction drag. By further heat addition, thrust could be developed to overcome other drags, such as the fuselage drag, and to accelerate the airplane. In all cases, the specific lift L/Q , according to linearized theory, remains unchanged.

Optimum wing profile angles and angle of attack. - Linear theory shows that large gains in L/Q can be obtained by simultaneously optimizing wing profile and angle of attack. The details of this development, which are given in appendix D, apply to the flat-top double-wedge airfoil. Figure 2(a) shows how the ratio of L/Q at angle of attack to the L/Q at zero angle of attack varies with the parameter angle of attack divided by the wing trailing-edge angle α/ϵ_2 . This particular parameter was chosen for the abscissa because it clearly shows that the L/Q ratio is unity for an angle of attack equal to the trailing-edge angle ϵ_2 as well as for zero angle of attack. The optimum angle of attack, where the L/Q ratio is a maximum, lies between these two values. Figure 2(b) shows that the lift coefficient (for a given Mach number and thickness) increases rapidly with angle of attack and at the optimum angle of attack is three times the value at zero angle of attack.

The flow deflection due to the heat-addition parameter $\epsilon_t/(\tau/c)$ also increases rapidly with angle of attack (fig. 2(b)). (Using ϵ_t rather than $\Delta T/T_0$ has the advantage of making the curves of figures 2

and 3 independent of flight Mach number except as Mach number, through β , appears in the parameters in the figures; ϵ_t is related to $\Delta T/T_0$ by eq. (B22).) The optimum angle of attack indicated in figure 2(a) is mathematically determinable (eq. (D10)), and the results presented in figure 3 are for this condition.

Figure 3(a) shows the L/Q ratio at optimum angle of attack as a function of the location of the maximum-thickness point of the wing, which is related to the ratio of the leading- to trailing-edge angles ϵ_1/ϵ_2 (eqs. (D7) and (D10)). The parameter $\beta C_D/(\tau/c)^2$ defines the amount of drag C_D over and above the drag due to the wing pressure forces that can be overcome. In this application C_D can also be thought of as an available thrust. If underwing heat addition is the sole means of propulsion and the flight configuration consists only of a wing, the value of C_D must be the coefficient of drag due to friction, which is equal to $2C_{fr}$. For a given ϵ_1/ϵ_2 , a low value of $\beta C_D/(\tau/c)^2$ is desirable for a high L/Q , which in turn suggests large thickness ratios, subject however to the limitations of the linearized theory. This thickness ratio will be called moderate.

When an airfoil has some thickness above the straight line joining the leading and trailing edges (topside thickness), the terms in the parameter $\beta C_D/(\tau/c)^2$ are defined as follows: τ/c is the bottom-side thickness ratio, and C_D includes the drag due to the topside thickness. Because small values of $\beta C_D/(\tau/c)^2$ give higher values of L/Q , a wing profile with a flat topside is desirable.

For all values of $\beta C_D/(\tau/c)^2$, the L/Q ratio gets indefinitely large as ϵ_1/ϵ_2 approaches zero (eq. (D6)); that is, when the wing maximum thickness is well downstream. It should be kept in mind that, for the linear theory to apply, all angles should be small; ϵ_1/ϵ_2 can be made small by choosing a small ϵ_2 and letting $\epsilon_1 \rightarrow 0$. The choice of ϵ_1 and ϵ_2 also affects the parameter $\beta C_D/(\tau/c)^2$, but through τ/c . For negative values of $\beta C_D/(\tau/c)^2$ shown in figure 3(b), large values of L/Q can also occur. Negative values of $\beta C_D/(\tau/c)^2$ mean that the thrust produced by heat addition is not sufficient to overcome the wing pressure drag. Low and negative values of $\beta C_D/(\tau/c)^2$ can be considered for propulsion using part ramjet and part underwing heat addition. The singularity for $\beta C_D/(\tau/c)^2 = -8$ corresponds to the overcoming of both wing friction and pressure drag by some propulsion other than underwing heat addition (see eq. (D13)). Because this singularity occurs at zero lift coefficient, as shown in figure 3(d), it is only of academic interest.

The optimum wing angle-of-attack parameters $\alpha/(\tau/c)$ corresponding to the curves of figures 3(a) and (b) are shown in figure 3(c). They also increase indefinitely as ϵ_1/ϵ_2 approaches zero. In spite of this, the trailing underside of the wing is always a downstream-facing surface.

The outstanding characteristic of the lift-coefficient parameter $\beta C_L/(\tau/c)$ shown in figure 3(d) is its increasing value with increasing drag-coefficient parameter $\beta C_D/(\tau/c)^2$. An example of the implication of this result is that an airplane with a high drag flies at a high C_L (i.e., a high altitude for a given wing loading W_G/S_w).

The deflection due to the heat-addition parameter $\epsilon_t/(\tau/c)$ is shown in figure 3(e). It increases with $\beta C_D/(\tau/c)^2$ similarly to the lift-coefficient parameter. There is also an infinitely large increase in the heat-addition parameter as ϵ_1/ϵ_2 approaches zero.

In summary, from the linearized theory, a wing designed for maximum L/Q will have the following characteristics: a moderate thickness ratio, a flat-top surface, and the maximum-thickness point of the wing well downstream. It should be operated at an optimum angle of attack. The heat addition is confined between the fore Mach waves from the under downstream portion of the wing.

Limitations on the linearized theory. - Figure 4 gives an idea of the magnitudes of $\Delta T/T_0$ of interest based on the linearized theory. (The linearized relation of $\Delta T/T_0$ to ϵ_t is given by eq. (B22).) Figure 4(a) indicates that, for maximum L/Q at $M = 8.0$ assuming turbulent boundary layer, values of $\Delta T/T_0$ above unity will be required. These values certainly exceed the limits of the linear theory, which assumes that this ratio is much less than unity. However, there are several ways to reduce these high values of $\Delta T/T_0$ in an attempt to get within the bounds of linear theory. From this figure, the value of $\Delta T/T_0$ can be reduced, for example, by choosing to design for minimum $\Delta T/T_0$. The resulting reduction in L/Q is moderate. Specifying operation at minimum $\Delta T/T_0$ also specifies the wing thickness ratio for a given skin-friction coefficient, as can be seen from the data in the figure. Also, $\Delta T/T_0$ can be reduced with moderate losses in L/Q by lowering the angle of attack from the optimum value, as can be seen from figure 2. Increasing ϵ_1/ϵ_2 will reduce $\Delta T/T_0$ but also L/Q , according to figures 3(a) and (e) (and eq. (B22)). An approximately minimum value of $\Delta T/T_0$ for a given friction coefficient occurs at $\alpha = 0$ (fig. 2(b)) and $\epsilon_1/\epsilon_2 = 1.0$ (fig. 3(e)).

These values are plotted in figure 4(t) as a function of friction coefficient for Mach numbers of 3 and 8. Noted on the curve are typical turbulent skin-friction coefficients. The minimum value of $\Delta T/T_0$ of interest at $M = 8.0$ for turbulent boundary layer is 0.2. For $\Delta T/T_0$ of 0.4 and a turbulent boundary layer, an L/Q twice the zero-angle-of-attack value may be attainable, according to linear theory.

Nonlinear Solutions

To ascertain the accuracy of the linearized solutions, a series of more rigorous calculations was made. The approach taken was to make calculations that were as simple as possible, and on wings suggested by the linearized theory. The heat was added in a plane (constant-area heat addition) normal to flow. The conditions across the plane of heat addition were calculated from the nonlinearized equations for the conservation of mass, momentum, and energy. The flow field downstream of the heat-addition plane was calculated by the method of characteristics.

Flat plate, zero angle of attack. - A typical flow field about and pressure distribution on a flat plate with heat addition are shown in figure 5 for $M = 8$ and $\Delta T/T_0 = 0.4$. For the more rigorous calculations (referred to in the figures as nonlinearized), the extent of the plateau of highest pressure rise is considerably less than the extent of pressure rise as calculated by the linear theory. Compensating for this in part, however, is the fact that the initial pressure rise is higher than that predicted by linear theory. Also, a significant pressure rise exists downstream of the initial plateau of high pressure and downstream of the distances βh and $2\beta h$.

The parameters L/Q and $C_L/(\Delta T/T_0)$ were computed from calculations like those of figure 5, for chord lengths of $c = \beta h$ and $c = 2\beta h$ (see abscissa of fig. 5), and a range of values of $\Delta T/T_0$ and M . The results are presented in figures 6 and 7. At $\Delta T/T_0 = 0$, L/Q has the linearized zero-angle-of-attack value. The variation of the linearized value of L/Q with Mach number is small, particularly at the higher Mach numbers. According to linearized theory, L/Q is independent of $\Delta T/T_0$. In the nonlinearized calculations, however, the L/Q drops rapidly from the linearized value with increasing $\Delta T/T_0$. For values of interest, say $\Delta T/T_0 = 0.4$, at $M = 8$, the L/Q is about 0.5 of the linearized zero-angle-of-attack value for $c = \beta h$ (fig. 6(a)). This factor of 0.5 may be compared with the factor of 2.0 previously discussed in the linearized theory for optimizing wing geometry to appreciate that it will be difficult to attain performance better than that of the zero-angle-of-attack linearized theory. The exact values of L/Q are higher for longer chord lengths (fig. 6(b)), but the larger chord lengths may not be practical because of the friction drag on the longer length. Irrespective of the

chord length, the deviation of the nonlinearized calculation from the linearized for a given $\Delta T/T_0$ increases with increasing free-stream Mach number.

Figure 7 presents corresponding plots of $C_L/(\Delta T/T_0)$. This parameter can be interpreted as the lift coefficient on a flat-plate wing of chord length c , or as the loading coefficient due to the heat addition on the portion of the wing affected by the heat addition. This parameter was chosen because it permits comparison with the linear theory. The deviation of $C_L/(\Delta T/T_0)$ from the linearized theory (the value of $\Delta T/T_0 = 0$) also increases with increasing $\Delta T/T_0$ and flight Mach number. The loading decreases for the longer lengths, as one would expect from figure 5. Both a high-loading C_L and high L/Q are necessary to achieve a high L/Q from an optimized wing. Increasing length has a favorable effect on L/Q but an unfavorable effect on C_L , and some compromise is required.

Heat distribution. - Three examples of heat-distribution configurations and their corresponding L/Q and C_L are taken from the previous calculations and together with a fourth case are presented in figure 8 to aid in discussing the effect of heat distribution. For all the cases, the total quantity of heat added to the stream is about the same. The point to be made by comparing cases A and B was discussed in the previous paragraph. The configuration of case C was synthesised from the previous calculation and has a heat-addition configuration very similar to that of case D. For case D the heat addition occurs in approximately equal quantities in two separate stream tubes of air. Both heat additions occur within the fore waves of the wing surface. For case D, note that the L/Q is nearly the same as for case C. The C_L is about doubled, as would be expected when the upstream wing surface in case C was removed and the pressures on the upstream surface were transmitted undiminished to the downstream surface. The heat distribution of case D yields a higher L/Q and C_L than the concentrated heat addition of case A.

Because both high L/Q and high C_L are desirable, it is concluded from these examples that distributing the heat so that the heat addition to any stream tube of air is small is desirable. The degree to which linearized theory can be approached by using a very large number of heat-addition steps of height h requires further study. Reference 5 concludes that distributing the heat so that $\Delta T/T_0 \rightarrow 0$ is of prime importance in getting good performance.

Wings. - Several wings at zero angle of attack, but with thickness and heat addition, were studied using the more rigorous calculation technique. Adding thickness to the underside of the wing reduced the L/Q from the zero-thickness case for a given $\Delta T/T_0$. For an example, at $M = 8.0$ for a $\Delta T/T_0 = 0.2$, the flat plate L/Q is 0.20; but, for a 2-percent-thick wing, with all the thickness on the underside, the L/Q is

0.187. This is due to the adverse effect of the expansion around the maximum-thickness point on the pressure rise that can be generated by heat addition on the downstream-facing area. Also, the effect of the increase in the speed of sound at the beginning of the heat addition due to the compression under the wing is adverse, as can be seen from equation (6a). The decrease in L/Q from the flat-plate value due to the flow turning after the heat addition, which is due to thickness (see fig. 1), appears to be a general result. No consideration was given to overcoming friction drag in this example.

The more rigorous calculations were also made at $M = 8.0$ for a series of wings with the general profiles and angles of attack suggested by the linear theory. The temperature-rise ratio (about 0.88) was chosen to make the Mach number after heat addition equal to 1.2, a convenient value for starting the characteristics net. The wings overcome the drag that is due to an estimated turbulent skin-friction coefficient of 0.00095. The results are presented in terms of L/Q in figure 9. Values of L/Q higher than the estimated flat-plate L/Q for the same $\Delta T/T_0$ were obtained. However, the best L/Q is very much less than that determined by linearized theory, as shown on the figure for one of the wings. The best L/Q is also considerably less than the linearized-theory zero-angle-of-attack value.

There are several modifications to the preceding calculation that would be expected to give some improvement in L/Q : (1) the use of an isentropic expansion surface to receive the high pressures due to the heat addition, (2) the use of a convex profile for the bottom upstream portion of the wing to reduce the turning angle after the heat addition, and (3) a refined balance between friction drag and lift due to heating to determine the optimum length of the trailing portion of the wing. The potential gains due to these modifications are not expected to be large.

On the basis of the linearized and more rigorous solutions presented, it appears that the linearized zero-angle-of-attack theory yields values of L/Q higher than are likely to be obtained by exact calculations for a wing with an optimized profile and attitude and having turbulent boundary layer and the heat addition concentrated near the wing. The best possibility for improving this performance is to distribute the heat so that on any streamline $\Delta T/T_0$ is very small.

Comparison with Ramjet

The analysis of the conventional wing plus ramjet used for purposes of comparison with the underwing heat addition is presented in appendix E.

Cruise performance. - A comparison of the cruise performance in terms of a range parameter $\frac{L}{Q} \left[\frac{V}{1 - \left(\frac{V}{V_s} \right)^2} \right]$ (see eq. (3)) as a function of

Mach number is shown in figure 10 for the case where either the ramjet or underwing heat addition is the sole means of propulsion. Two curves (C and D) are shown for the performance of underwing heat addition. Curve D was drawn through the best performance calculated by the rigorous technique (from fig. 9) by using the linearized theory as a guide to draw the Mach number variation. The curve represents about the best that can be done by optimizing wing geometry when concentrated heat addition is used. Curve C represents a performance that may possibly be achieved if the wing geometry is optimized and a distributed heat is used (i.e., $\Delta T/T_0 \rightarrow 0$). The curve was calculated assuming a performance of twice the linearized zero-angle-of-attack value (see fig. 3(a) or 4(a)). The predominant trend of both curves is the increase in range with flight Mach number. A comparison of the curves shows the wide uncertainty in the performance of underwing heat addition and indicates the importance that heat distribution may have.

Two curves (A and B) are also shown for the conventional wing plus ramjet. Curve A assumes more optimistic values of aerodynamic and thermodynamic performance, while curve B has more conservative assumptions. Again a significant point to be observed from these two curves is the wide difference in range performance, particularly at the higher Mach numbers, due to the difference in assumptions. A major cause of the decrease in range parameter at the higher Mach numbers for ramjet curve B is the assumption of a limiting temperature rise, in that the $\Delta T/T_0$ at the higher Mach numbers decreases, as is shown by the auxiliary abscissa.

If high temperature-rise ratios are required for underwing heat addition as is indicated in figure 4(a) for a concentrated heat addition, then the range performance of curve D should also drop off at the higher Mach numbers, although the curve does not show this. An interesting difference between the ramjet and underwing heat addition is that, as the flight Mach number increases, good ramjet performance depends on maintaining a high temperature rise (about unity) in the air handled by the engine, while good performance of underwing heat addition at any Mach number appears to depend on achieving a very low temperature rise in a large quantity of air.

Although the degree of uncertainty in making these range comparisons is large, the following conclusions are warranted:

- (1) Underwing heat addition is most likely to be competitive on a range basis with the conventional wing plus ramjet at the higher supersonic Mach numbers.

(2) For underwing heat addition restricted to the region adjacent to the wing, the conventional wing plus ramjet is superior to underwing heat addition on an aerothermodynamic basis below about $M = 8.0$.

(3) The best hope for improving the performance of underwing heat addition seems to lie in the distribution of the heat under the wing.

Considered in figure 11 is the cruise performance of systems using combinations of ramjet propulsion and underwing heat addition. (The details of the analysis are given in appendix F.) Over-all L/Q is plotted as a function of the fraction of the total heat input consumed by the ramjet in figure 11(a). When the parameter is zero, underwing heat addition is the sole means of propulsion. The value shown for this condition is the linearized-theory value for the high-performance wing shown in the sketch. Providing some of the propulsion by ramjet and re-optimizing the wing angle of attack for the reduced underwing heat addition result in a net decrease in the over-all L/Q .

For a value of the abscissa of unity, all the propulsion is provided by the ramjet. The optimum wing shape for a given thickness is double wedge with half the thickness on the top side of the wing. Adding a small amount of heat under the wing decreases the over-all L/Q . This occurs in spite of the fact that the underwing heat addition potentially has a higher L/Q . The physical reason for this result is suggested by the wing sketches. For example, for the optimum wing propelled by a ramjet, the "under downstream" surface faces upstream. The first increment of heat addition thus contributes drag as well as lift. For the optimum wing with underwing heat addition, the "under downstream" surface always faces downstream, so that heat addition produces thrust. The wing profiles that are optimum for underwing heat addition and for no heat addition are so different that trying to combine the two systems results only in reduced performance.

If the ramjet performance is poor enough compared with underwing heat addition, a point is reached where small additions of underwing heat will improve performance. Under this condition a pure underwing-heat-addition system would be still better. In general, in no case does the composite system performance exceed that of the better single system. The previous comparison of the pure systems in figure 10 is thus a general evaluation.

Airplane weights as well as L/Q affect airplane range. Shown in figure 11(b) are the operating lift coefficients for the wings of figure 11(a). For pure underwing heat addition the operating lift coefficient is about twice that for the optimum wing with pure ramjet propulsion. This increased lift coefficient reduces the required wing size by about half. In general, for a given airplane gross weight, wing thickness ratio, and fiber stress, the wing weight varies as the square root of the

wing area. Thus halving the wing area reduces its weight about 30 percent. The weight chargeable to the propulsion system should also be substantially decreased by underwing heat addition. An example of the effect of these weight changes on range, using arbitrary but reasonable numbers, is as follows:

	Ramjet system	UWHA system
Ratio of wing to initial gross weight	0.12	0.085
Ratio of engine to initial gross weight	.06	.01
Ratio of fuel to initial gross weight	.60	.685
Relative range	1.00	1.26

This example shows a 26-percent gain in range due to savings in wing and engine weight by using underwing heat addition. Large or small fuel weight ratios will emphasize the effect of a weight change on relative range. This weight effect on range is multiplied with the L/Q effect. Compared with the uncertainties of the aerothermodynamic performance shown in figure 10, the weight effect is not large.

Maneuver performance. - The possibility of using underwing heat addition for maneuvering is also most clearly explained by an example. It is assumed that an airplane is designed for maximum range at $M = 8.0$ (the altitude, wing size, and engine size all having been optimized) and that this airplane is also required to maneuver at the cruise altitude without loss of speed or altitude. The required maneuverability can be achieved by increasing the size of the ramjet engines. The increased engine size forces the design away from the optimum conditions during cruise, with a concomitant decrease in range. The loss in range is indicated in figure 12(a) by the decrease in L/Q that occurs if the wing size is unchanged but the cruise altitude is reoptimized. (The increase in engine weight, which would also decrease range, has not been accounted for. Increasing wing size could improve the L/Q , but the increased wing weight would cause a net decrease in range.) If the required maneuverability is obtained by underwing heat addition, the optimum cruise design need not be compromised.

The maneuver L/Q using a ramjet sized for maneuvering is given in figure 12(b). In this case the wing now goes off design, so that the maneuver L/Q decreases with increasing maneuverability. This is compared with the L/Q attainable with underwing heat addition as determined from figures 6(a) and 7(a), which are results of the more rigorous calculations. The maneuvering L/Q is lower for underwing heat addition. However, the important point is that using underwing heat addition for maneuvering avoids compromising the cruise performance of the missile, as indicated in figure 12(a). A major fraction of the airplane fuel is usually used in cruise, and hence this the phase of the flight that should

be kept efficient. (Maneuverability here can be interpreted as a short-time high-altitude capability. An airplane designed for cruise can maneuver at a decreased altitude; for example, $n = 4$ g's can be attained at an altitude about 30,000 ft below cruise altitude.) The example discussed illustrates that underwing heat addition can be advantageously combined with a conventional wing-plus-ramjet cruise airplane to achieve maneuverability at or above cruise altitude at high Mach numbers. An analysis of each specific airplane design problem is required to determine whether underwing heat addition will be an advantage in each case.

Qualitative considerations. - There are characteristics of underwing heat addition that have not been evaluated in this report that are important. At high flight Mach numbers the convective heat input from the high-pressure hot gases within the engine poses a severe problem in terms of cooling to be provided and/or high materials temperatures. With underwing heat addition, it is possible in principle to derive the required propulsion by heating air that is not in contact with any structural surfaces and with static pressures on structural surfaces lower than those in a ramjet, thus minimizing the convective heat input. In addition, because there are no enclosed areas, all the airplane surfaces would have the opportunity to cool by radiation. If underwing heat addition can be used at higher Mach numbers than the conventional ramjet, this in turn would influence the range comparison, as can be seen from figure 10.

If the required supersonic heat addition is considered to result from fuel injection and combustion, adding heat spread out along the fore Mach wave from the under trailing portion of the wing appears to be a difficult practical problem, in that such devices as spray bars will probably cause a prohibitive drag. Three-dimensional or "end" effects will generally cause a reduction in performance from the two-dimensional value. The losses due to end effects will increase with the distance of the heat addition from the wing.

In the conventional ramjet, with subsonic combustor velocities, high static temperatures cause dissociation of the working gases, which may have an adverse effect on ramjet efficiency. If this is a major problem, supersonic combustor velocities may be considered for the ramjet. Underwing burning, on the other hand, tends to operate at lower static temperatures and thus minimizes the dissociation problem. The static temperature will depend on the Mach number after heat addition, or the $\Delta T/T_0$ and the distribution of the heat.

With the conventional ramjet, operation over a range of flight Mach numbers requires mechanically difficult geometry changes. An underwing-heat-addition configuration would avoid this problem.

Exotic means of heating such as nuclear or electromagnetic may influence the usefulness of underwing heat addition.

SUMMARY OF RESULTS

The linearized theory for heat addition under a wing has been developed to optimize wing geometry, heat addition, and angle of attack. The optimum wing has all of the thickness on the underside of the airfoil, with maximum-thickness point well downstream, has a moderate thickness ratio, and operates at an optimum angle of attack. The heat addition is confined between the fore Mach waves from the under trailing surface of the wing. By linearized theory a wing at optimum angle of attack may have a range efficiency about twice that of a zero-angle-of-attack wing.

More rigorous calculations using the method of characteristics for particular flow models were made for heating under a flat-plate wing and for several wings with thickness, both for heat additions concentrated near the wing. The more rigorous calculations yield in practical cases efficiencies about half of those estimated by linear theory. An analysis of distributing the heat addition between the fore waves from the under-trailing portion of the wing indicates this is a way of improving the performance, and further calculations appear desirable.

A comparison of the conventional ramjet plus wing with underwing heat addition when the heat addition is concentrated near the wing shows the former to be superior on a range basis up to Mach number of about 8. The heat distribution under the wing and the assumed ramjet and airframe performance may have a marked effect on this conclusion. Underwing heat addition can be useful in providing high-altitude maneuver capability at high flight Mach numbers for an airplane powered by conventional ramjets during cruise.

Lewis Research Center
National Aeronautics and Space Administration
Cleveland, Ohio, December 23, 1958

APPENDIX A

SYMBOLS

A_0	free-stream tube of air
a	speed of sound
C_D	defines drag over and above the drag due to wing pressure forces that can be overcome; or $2C_{fr}$ plus drag coefficients of airplane components other than wing, based on wing area
$C_{D,i}/C_L^2$	drag due to lift parameter
C_{fr}	wing friction coefficient based on wetted area
C_L	coefficient of lift based on wing chord (except in eq. (6b)), $L/(\gamma/2)pM_c^2$
$\left(\frac{dC_L}{d\alpha}\right)$	lift-curve slope
C_V	exhaust-nozzle velocity coefficient
c	chord of airfoil
c_p	specific heat at constant pressure
D	drag force
F	thrust force
g	acceleration due to gravity
h	heating value of fuel, Btu/lb
I	thrust specific impulse, F/w_f
J	mechanical equivalent of heat, 778 ft-lb/Btu
L	lift force
L/D	airplane lift-drag ratio
M	free-stream Mach number

n	maneuvering acceleration, normal to plane of wing span and velocity vector, in g's; n = 1 for level flight
p	static pressure
Q	total rate of heat release, hw_f , Btu/sec
R	gas constant
α	range
T	total temperature, $^{\circ}R$
ΔT	temperature rise due to heat addition, $^{\circ}R$
t	static temperature, $^{\circ}R$
v	flight velocity
v_s	satellite velocity taken as 26,000 ft/sec
w_f/w_G	ratio of fuel weight to airplane gross weight
w_G/S_w	wing loading, airplane gross weight/wing plan area
w_a	weight of airflow per second
w_f	weight of fuel flow per second
α	angle of attack, deg
α_M	Mach angle
β	$\sqrt{M^2 - 1}$
γ	ratio of specific heats
ϵ	wing angles (see fig. 1)
η_e	inlet kinetic-energy efficiency
θ	total-temperature ratio
λ	turning angle (see appendix B and fig. 13)
τ	wing thickness
Ω	maneuver total turning angle, deg

Subscripts:

c	at cruise conditions
l	linearized theory (in general at angle of attack)
$l, \alpha=0$	linearized theory at zero angle of attack
max	maximum
n	during maneuver
opt	value at maximum lift-drag ratio (no heat addition)
r	refers to ramjet
t	total turning angle due to heat addition
u	refers to underwing heat addition
0	free-stream conditions

APPENDIX B

ENGINEERING DERIVATION OF EFFECT OF SUPERSONIC
UNDERWING HEAT ADDITION

This appendix is divided into several sections that discuss in turn the basic effects of supersonic heat addition, the performance of the double-wedge wing at zero angle of attack without and with friction drag, and the wing lift coefficients.

Basic Considerations of Supersonic Heat Addition

The efficiency of underwing heat addition is evaluated in terms of a specific lift parameter defined as the lift per Btu per second:

$$\frac{L}{Q} = \frac{L}{hw_f} \quad (1)$$

The following assumptions are made in the analysis: small angles, small intensity of heat addition, and constant specific heats and molecular weight. The variables to be evaluated in equation (1) are L and w_f or Q . This derivation follows directly the approach of reference 1. Consider the problem illustrated in figure 13(a) for a small-intensity constant-area heat addition. The equations for the conservation of momentum and mass are

$$p(1 + \gamma M^2) = K_1 \quad (B1)$$

$$\frac{\gamma p M}{a} = K_2 \quad (B2)$$

The definition of the speed of sound and the equation for the total temperature are

$$a = (\gamma g R t)^{1/2} \quad (B3)$$

$$T = t \left(1 + \frac{\gamma - 1}{2} M^2 \right) \quad (B4)$$

Using these equations in differential form, the static-pressure rise through constant-area heat addition is

$$\frac{dp}{p_0} = \frac{\left(1 + \frac{\gamma - 1}{2} M^2 \right) \gamma M^2}{M^2 - 1} \frac{dT}{T_0} \quad (B5)$$

The corresponding change in Mach number is

$$dM = - \frac{1 + \gamma M^2}{2\gamma M} \frac{dp}{p_0} \quad (B6)$$

If the heat addition is thought of as occurring in a plane (or line) as in figure 13(d), then constraining walls are not required for the assumption of constant-area heat addition to apply.

By linearized theory the static-pressure change due to a flow deflection is

$$\frac{dp}{p_0} = \frac{\gamma M^2 \lambda}{\sqrt{M^2 - 1}} \quad (B7)$$

and this is illustrated in figure 13(b).

If the static-pressure rise due to heat addition is expanded back to the original free-stream pressure, the expansion angle is given by the combination of equations (B5) and (B7):

$$\lambda = \frac{1 + \frac{\gamma - 1}{2} M^2}{\sqrt{M^2 - 1}} \frac{d\Gamma}{T} \quad (B8)$$

This case is illustrated in figure 13(c). The pressure rise due to heat addition is now limited in the downstream direction by the Mach wave from the turn λ . Equation (B8) defines the parameter $\epsilon_t = \lambda$ used in the following section of this appendix and in the body of the report.

If the flow after heat addition is exhausted side by side with the free stream, a pressure balance is struck between the two streams so that the deflection angle is half the angle that exists if the flow were expanded back to free-stream static pressure. Also, the pressure rise at the interface between the heated and the free streams is half the pressure rise due to heat addition in a constant-area duct. This case is illustrated in figure 13(d). (This is the same result given by eq. (11d) of ref. 1 if the term multiplied by the $(\Delta Q_2/Q_2)\Delta\alpha$, which is second-order, is neglected.)

The preceding relations can be considered to define an effective λ for the effect of temperature change (eq. (B8)) and pressure change (eq. (B7)). Of course, λ itself represents the effect of flow turning. This point of view is taken in the following development.

Derivation of Performance of Flat-Top Double-Wedge

Airfoil at Zero Angle of Attack Without Friction

The application of these concepts to a wing with heat addition, shown in figure 1, will now be considered, first for the case neglecting friction effects. The parameter

$$\frac{L}{Q} = \frac{L}{hw_f} \quad (1)$$

will be considered for the case of thrust equal to drag. The thrust force, in terms of a coefficient referred to p_0 and c , on the trailing portion of the wing due to external combustion, is

$$\frac{F_2}{p_0 c} = \frac{p_2 - p_0}{p_0} \frac{\tau}{c} = \frac{\Delta p_2}{p_0} \frac{\tau}{c} \quad (B9)$$

The effective angle due to heat addition required to keep the pressure equal to p_0 on the trailing surface is, from the considerations leading to equation (B7) and from figure 1, ϵ_2 . The effective angle due to heat addition to produce a given pressure rise above p_0 on the trailing surface is designated ϵ_3 . The pressure rise due to ϵ_3 is given by equation (B7):

$$\frac{\Delta p_2}{p_0} = \frac{\gamma M^2}{\sqrt{M^2 - 1}} \epsilon_3 \quad (B10)$$

Hence, the thrust coefficient for the trailing portion of the wing becomes

$$\frac{F_2}{p_0 c} = \frac{\gamma M^2}{\sqrt{M^2 - 1}} \frac{\tau}{c} \epsilon_3 \quad (B11)$$

The total turning due to heat addition to get this thrust coefficient is

$$\epsilon_t = \epsilon_2 + \epsilon_3 \quad (B12)$$

The pressure drag on the leading portion of the wing, for no heat addition under the leading portion, is by similar considerations

$$\frac{D_1}{p_0 c} = \frac{\Delta p_1}{p_0} \frac{\tau}{c} = \frac{\gamma M^2}{\sqrt{M^2 - 1}} \frac{\tau}{c} \epsilon_1 \quad (B13)$$

where, by equation (B6),

$$\frac{\Delta p_1}{p_0} = \frac{\gamma M^2}{\sqrt{M^2 - 1}} \epsilon_1 \quad (B14)$$

Equating the thrust with the drag gives

$$\epsilon_3 = \epsilon_1 \quad (B15)$$

The lift on the configuration is

$$\frac{L}{p_0 c} = \frac{\Delta p_1}{p_0} \frac{\epsilon_2}{\epsilon_1 + \epsilon_2} + \frac{\Delta p_2}{p_0} \frac{\epsilon_1}{\epsilon_1 + \epsilon_2} \quad (B16)$$

Using the previous values for $\Delta p_1/p_0$ and $\Delta p_2/p_0$,

$$\frac{L}{p_0 c} = \frac{\gamma M^2}{\sqrt{M^2 - 1}} \frac{\epsilon_1(\epsilon_2 + \epsilon_3)}{\epsilon_1 + \epsilon_2} \quad (B17)$$

and using equation (B15) or (B12),

$$\frac{L}{p_0 c} = \frac{\gamma M^2 \epsilon_1}{\sqrt{M^2 - 1}} = \frac{\gamma M^2}{\sqrt{M^2 - 1}} \frac{\epsilon_1 \epsilon_t}{\epsilon_1 + \epsilon_2} \quad (B18)$$

The quantity of heat added will now be calculated. The amount of air being heated is

$$w_a = \frac{g \gamma p_0 M A_0}{a} \quad (B19)$$

but, from figure 1,

$$A_0 = \frac{\epsilon_1 c}{\epsilon_1 + \epsilon_2} \tan \alpha_M = \frac{\epsilon_1 c}{\epsilon_1 + \epsilon_2} \frac{1}{\sqrt{M^2 - 1}} \quad (B20)$$

so that

$$w_a = \frac{g \gamma p_0 M}{a \sqrt{M^2 - 1}} \frac{\epsilon_1 c}{\epsilon_1 + \epsilon_2} \quad (B21)$$

The temperature rise to give the pressure desired on the trailing portion of the wing is, by equation (B8),

$$\frac{\Delta T}{T_0} = \frac{\sqrt{M^2 - 1}}{1 + \frac{\gamma - 1}{2} M^2} \epsilon_t \quad (B22)$$

The quantity of heat added is

$$Q = c_p w_a \Delta T \quad (B23)$$

and, in a coefficient form, using equations (B21), (B22), and (B4),

$$\frac{Q}{p_0 c} = \frac{c_p g r M t}{a} \frac{\epsilon_l \epsilon_t}{\epsilon_l + \epsilon_2} \quad (B24)$$

The specific lift thus becomes, from equations (B18) and (B24),

$$\frac{L}{Q} = \frac{a}{c_p g t} \frac{M}{\sqrt{M^2 - 1}} = \frac{(\gamma - 1) J}{a} \frac{M}{\sqrt{M^2 - 1}} \quad (B25)$$

Equation (B25) is used as a reference value for the analysis in appendix D. Note that the effect of wing thickness has dropped out, so that the specific lift is independent of the thickness and bottom profile within the restrictions of small angles. This result must then hold also for a flat plate. Also, the specific lift is independent of the intensity of the heat addition, again as long as it is small.

Derivation of Performance of Flat-Top Double-Wedge

Airfoil at Zero Angle of Attack with Friction

The problem of other airplane drags and of wing friction assuming the friction drag is unchanged by the heat addition will now be considered. The drag previously given by equation (B13) can for this case be written

$$\frac{D}{p_0 c} = \left(\frac{\frac{\tau}{c} \epsilon_1}{\sqrt{M^2 - 1}} + \frac{C_D}{2} \right) \gamma M^2 \quad (B26)$$

where $C_D = 2C_{fr}$ plus the drag coefficients of other airplane components based on the wing plan area. Equating the thrust (eq. (B11)) to the drag gives

$$\epsilon_3 = \epsilon_1 + \frac{C_D \sqrt{M^2 - 1}}{2\tau/c} \quad (B27)$$

The pressure rise on the trailing portion of the wing is still given by equation (B10), and the lift is still given by equations (B16) to (B18). Hence, the specific lift is independent of the friction drag on the wing and of the other airplane drags.

Lift Coefficients for Wings at Zero Angle of Attack with Heat Addition

The wing lift coefficient, defined as

$$C_L = \frac{L}{\frac{\rho}{2} p_0 M^2 c} \quad (B28)$$

is, from equation (B18) for the case assuming no friction,

$$C_L = \frac{2\epsilon_1}{\sqrt{M^2 - 1}} \quad (B29)$$

The lift coefficient for the case with friction is given by equations (B17) and (B27):

$$C_L = \frac{2\epsilon_1 \left(\epsilon_1 + \epsilon_2 + \frac{C_D \sqrt{M^2 - 1}}{2\tau/c} \right)}{\sqrt{M^2 - 1} (\epsilon_1 + \epsilon_2)} \quad (B30)$$

These lift coefficients may be compared with that for the conventional wing given by equation (E10). Note that for a given wing geometry the operating lift coefficient for the case with friction is higher than for the case without friction. To support a given weight at a given altitude, a smaller wing is required for the case with friction. These developments have been for thrust equal to drag. From equation (B29) the lift coefficient goes to zero if the thickness (ϵ_1) goes to zero.

The lift coefficient due to heat addition on a zero-angle-of-attack flat plate without regard to thrust production can also be considered.

The lift coefficient based on the length of chord over which the lifting pressures act is

$$C_L = \frac{L}{\frac{\gamma}{2} p_0 M^2 c} = \frac{\Delta p}{\frac{\gamma}{2} M^2 p_0} \quad (B31)$$

which, from equation (B5), becomes

$$C_L = \frac{2(1 + \frac{\gamma - 1}{2} M^2)}{M^2 - 1} \frac{\Delta T}{T_0} \quad (B32)$$

This may also be interpreted as an increment in lift coefficient due to heat addition, which can be added to the lift coefficient due to angle of attack. This is the same result given by equation (B18), where

$\frac{c\epsilon_1}{\epsilon_1 + \epsilon_2}$ is the chord on which the lift due to heating acts and on which the lift coefficient of equations (B31) and (B32) is based.

APPENDIX C

DERIVATION OF EFFECT OF SUPERSONIC UNDERWING HEAT
ADDITION FROM POTENTIAL-FLOW EQUATIONS

By Stephen H. Maslen

The equations for inviscid motion with heat addition are

$$\left. \begin{aligned} \frac{\partial}{\partial x} (\rho u) + \frac{\partial}{\partial y} (\rho v) &= 0 \\ \rho \left(u \frac{\partial u}{\partial x} + v \frac{\partial u}{\partial y} \right) + \frac{\partial p}{\partial x} &= 0 \\ \rho \left(u \frac{\partial v}{\partial x} + v \frac{\partial v}{\partial y} \right) + \frac{\partial p}{\partial y} &= 0 \\ \rho c_p \left(u \frac{\partial t}{\partial x} + v \frac{\partial t}{\partial y} \right) - \left(u \frac{\partial p}{\partial x} + v \frac{\partial p}{\partial y} \right) &= q \\ p &= \rho R t \end{aligned} \right\} \quad (C1)$$

where q is the heat added per unit volume per unit time, x, y and η, ζ are coordinate systems, u and v are velocity components, and ρ is density. Assuming a small heat addition and a thin low-angle-of-attack wing, equations (C1) can be solved by linearized theory. The variation in the molecular weight and specific heat due to burning is ignored.

A velocity potential ϕ can be defined so that

$$u = u_0 + \frac{\partial \phi}{\partial x}$$

$$v = \frac{\partial \phi}{\partial y}$$

where the subscript 0 refers to free-stream conditions. Equations (C1) can then be expanded for small variation from the undisturbed state. After some rearrangement, one obtains finally

$$\beta^2 \frac{\partial^2 \phi}{\partial x^2} - \frac{\partial^2 \phi}{\partial y^2} = - \frac{q}{\rho_0^2 c_p t_0} \quad (C2)$$

The general integral of this equation, assuming that all the burning is under the wing, is

$$\varphi = f(x + \beta y) + f(x - \beta y) + \frac{1}{2\rho_0 \beta c_p t_0} \left[\int_0^y d\eta \int_0^{x+\beta(y-\eta)} q(\zeta, \eta) d\zeta + \int_y^{y-x/\beta} d\eta \int_0^{x-\beta(y-\eta)} q(\zeta, \eta) d\zeta \right] \quad (C3)$$

The quantities f and f' are arbitrary functions of their arguments. The wing is assumed to be near the plane $y = 0$, extending from $x = 0$ to $x = c$. The function f' corresponds to waves from infinity upstream and so is identically zero. The remaining function f can be found from the boundary condition at the wing surface. The problem is linear and can therefore be solved by superposition of solutions. If the present effect is merely that of the burning, then the boundary condition is that

$$v(x, 0) = \left(\frac{\partial \varphi}{\partial y} \right)_{x, 0} = 0$$

Hence

$$\frac{\partial f(x)}{\partial x} = \frac{1}{2\rho_0 \beta c_p t_0} \int_0^{-x/\beta} q(x + \beta \eta, \eta) d\eta$$

so that

$$f(x + \beta y) = \frac{1}{2\rho_0 \beta c_p t_0} \int_0^{-\frac{x+\beta y}{\beta}} d\eta \int_0^{x+\beta \eta + \beta y} q(\zeta, \eta) d\zeta$$

Thus, finally, from equation (C3),

$$\begin{aligned} \varphi = & \frac{1}{2\rho_0 \beta c_p t_0} \left[\int_0^{-\frac{x+\beta y}{\beta}} d\eta \int_0^{x+\beta y + \beta \eta} q(\zeta, \eta) d\zeta + \right. \\ & \left. \int_0^y d\eta \int_0^{x+\beta(y-\eta)} q(\zeta, \eta) d\zeta + \int_y^{y-(x/\beta)} d\eta \int_0^{x-\beta(y-\eta)} q(\zeta, \eta) d\zeta \right] \end{aligned} \quad (C4)$$

The pressure coefficient ψ on the underside of the wing, due to the burning, is

$$\psi = - \frac{2}{u_0} \left(\frac{\partial \varphi}{\partial x} \right)_{y=0} = \frac{2}{\rho_0 u \beta c_p t_0} \int_{-x/\beta}^0 q(x + \beta \eta, \eta) d\eta \quad (C5)$$

Also

$$\varphi(x, 0) = \frac{1}{\rho_0 \beta c_p t_0} \int_{-x/\beta}^0 d\eta \int_0^{x+\beta \eta} q(\zeta, \eta) d\zeta \quad (C6)$$

The lift due to burning is given by

$$\begin{aligned} L &= \frac{1}{2} \rho_0 u_0^2 \int_0^c \psi dx = - \rho_0 u_0 [\varphi(c, 0) - \varphi(0, 0)] \\ &= \frac{u_0}{\beta c_p t_0} \int_{-c/\beta}^0 d\eta \int_0^{c+\beta \eta} q(\zeta, \eta) d\zeta \end{aligned} \quad (C7)$$

but the total rate of heat release Q in the region forward for the Mach line going upstream from the trailing edge is

$$Q = \int_{-c/\beta}^0 d\eta \int_0^{c+\beta \eta} q(\zeta, \eta) d\zeta \quad (C8)$$

Thus, finally,

$$\frac{L}{Q} = \frac{Ju_0}{\beta c_p t_0} = \frac{(r-1)JM}{a\sqrt{M^2-1}} \quad (C9)$$

the J being introduced so that the lift is in pounds and the heat in Btu per second. The equation is identical with equation (B25). Thus, as far as lift is concerned, any heat added between the forward Mach line from the leading and trailing edges is effective. Within this limit, the point at which the heat is added is immaterial.

As for the drag increment, this is

$$D = \frac{1}{2} \rho_0 u_0^2 \int_0^l \psi(x) \sin \delta(x) dx \quad (C10)$$

where the pressure coefficient is given by equation (C5), and δ is the local inclination of the wing under surface with respect to the free stream. It is thus apparent that the burning should occur aft of the Mach line forward from the maximum-thickness point (see fig. 1, e.g.) if one wants a maximum thrust from the burning. This is true because the pressure increment on the wing due to burning is everywhere positive (eq. (C5)). For example, if heat Q_I is released in region I of figure 1, then for the wing of that figure there is obtained from equations (C10), (C7), and (C9),

$$\frac{D}{Q} = \left[(\epsilon_1 + \alpha) \frac{Q_I}{Q} - (\epsilon_2 - \alpha) \frac{Q_{II}}{Q} \right] \frac{(\gamma - 1)JM}{a\sqrt{M^2 - 1}}$$

Thus, as far as minimizing drag is concerned, Q_I should vanish.

APPENDIX D

OPTIMUM WING ANGLE OF ATTACK AND PROFILE ANGLES

This appendix uses the linearized theory to discuss wing angle of attack and shape to maximize L/Q . By use of the approach developed in appendix B, the equations for the lift, drag, thrust, and heat addition may be written respectively as follows:

$$\frac{L}{P_0 C} = \frac{\gamma M^2}{\beta} \left[\alpha + \frac{\epsilon_2(\epsilon_1 + \alpha)}{\epsilon_1 + \epsilon_2} + \frac{\epsilon_1(\alpha - \epsilon_2 + \epsilon_t)}{\epsilon_1 + \epsilon_2} \right] = \frac{\gamma M^2}{\beta} \left[2\alpha + \frac{\epsilon_1 \epsilon_t}{\epsilon_1 + \epsilon_2} \right] \quad (D1)$$

$$\frac{D}{P_0 C} = \frac{\gamma M^2}{\beta} \left[\alpha^2 + \frac{\epsilon_2(\epsilon_1 + \alpha)^2}{\epsilon_1 + \epsilon_2} + \frac{\beta C_D}{2} \right] \quad (D2)$$

$$\frac{F}{P_0 C} = \frac{\gamma M^2}{\beta} \left[\frac{\epsilon_1(\epsilon_2 - \alpha)(\alpha - \epsilon_2 + \epsilon_t)}{\epsilon_1 + \epsilon_2} \right] \quad (D3)$$

$$\frac{Q}{P_0 C} = \frac{c_p g \gamma M t}{a} \left(\frac{\epsilon_1 \epsilon_t}{\epsilon_1 + \epsilon_2} \right) \quad (D4)$$

Equation (D1) shows the superposition of the lift due to angle of attack and due to heat addition that results from the linearized-theory assumptions. Equating the thrust to the drag gives

$$\epsilon_t = \frac{\epsilon_1 + \epsilon_2}{\epsilon_1} \left(\frac{2\alpha^2 + \epsilon_1 \epsilon_2 + \frac{\beta C_D}{2}}{\epsilon_2 - \alpha} \right) \quad (D5)$$

Forming the ratio of the L/Q at angle of attack $(L/Q)_l$ to the value at zero angle of attack $(L/Q)_{l,\alpha=0}$ (eq. (C9) or (B25)) and combining equations (D1), (D4), and (D5) give

$$\frac{(L/Q)_l}{(L/Q)_{l,\alpha=0}} = 1 + \frac{2\alpha(\epsilon_l - \alpha)}{2\alpha^2 + \epsilon_1 \epsilon_2 + \frac{\beta C_D}{2}} \quad (D6)$$

Letting $\alpha = k\epsilon_2$, $\epsilon_1 = l\epsilon_2$, and $B = \frac{\beta C_D}{2\left(\frac{l}{c}\right)^2}$, equation (D6) becomes

$$\frac{(L/Q)_l}{(L/Q)_{l,\alpha=0}} = 1 + \frac{2k(l - k)}{2k + l + B \left(\frac{l}{1+l} \right)^2} \quad (D7)$$

and equation (D5) becomes

$$\frac{\epsilon_t}{\left(\frac{\tau}{c}\right)} = \frac{\left(\frac{1+l}{l}\right)^2 (2k^2 + l) + B}{1 - k} \quad (D8)$$

The lift coefficient, defined as

$$C_L = \frac{L}{\frac{\gamma}{2} p M_c^2} \quad (B28)$$

is determined from equation (D1) and is

$$\frac{\beta C_L}{\left(\frac{\tau}{c}\right)} = 2 \left[2k \left(\frac{1+l}{l} \right) + \frac{\epsilon_t}{\tau/c} \left(\frac{l}{1+l} \right) \right] \quad (D9)$$

Equation (D7) may be optimized with respect to $k = \alpha/\epsilon_2$ to give

$$k_{opt} = \left[\frac{l + B \left(\frac{l}{1+l} \right)^2}{2} \right] \left[\sqrt{1 + \frac{2}{l + B \left(\frac{l}{1+l} \right)^2}} - 1 \right] \quad (D10)$$

The angle of attack is related to the thickness ratio by $\frac{\alpha}{\tau/c} = k \left(\frac{1+l}{l} \right)$.

Significant parameters from the preceding development are plotted in figure 3 and discussed in the body of the report.

The approximate minimum value for $\epsilon_t/(\tau/c)$ is shown in figures 2(b) and 3(e) to occur at $\alpha = 0$ and $\epsilon_1/\epsilon_2 = 1.0$. The minimum value C_D can have is $2C_{fr}$. Differentiating equation (D8) with respect to τ/c to minimize ϵ_t gives

$$\frac{\tau}{c} = \frac{\sqrt{\beta C_{fr}}}{2} \quad (D11)$$

and finally equation (D8) gives for the minimum value of ϵ_t

$$\epsilon_t = 4 \sqrt{\beta C_{fr}} \quad (D12)$$

The parameters $\Delta T/T_0$ and ϵ_t are related by equation (B22). A plot of the temperature-rise ratio $\Delta T/T_0$ associated with several friction coefficients is given in figure 4(b) and discussed in the body of the report.

For the wing defined by $\alpha = 0$, $\epsilon_1/\epsilon_2 = 1.0$, and having a flat top, the pressure drag for no underwing heat addition is

$$C_{D,p} = \frac{8(\tau/c)^2}{\beta} \quad (D13)$$

This is equal to the friction drag $C_{D,fr} = 2C_{fr}$ of the wing, according to equation (D11).

APPENDIX E

PERFORMANCE OF CONVENTIONAL WING PLUS RAMJET

The thrust coefficient C_F for a conventional ramjet may be written (by ref. 10) as

$$C_{F,A_0} = 2(C_V \sqrt{\theta \eta_e} - 1) \quad (E1)$$

where C_{F,A_0} is defined by

$$C_{F,A_0} = \frac{F}{\frac{\gamma}{2} p_0 M^2 A_0}$$

For an ideal gas,

$$\theta = 1 + \frac{\Delta T}{T_0} = 1 + \frac{\Delta T}{t \left(1 + \frac{\gamma - 1}{2} M^2 \right)} \quad (E2)$$

A value of $\Delta T/T_0 = 1.0$ or $\theta = 2.0$ is generally near optimum and was used in one set of assumptions. A temperature rise ΔT of $4000^\circ R$ is about what is possible with hydrocarbon fuels, and this value was used in a second set of assumptions. As can be seen from the auxiliary abscissa in figure 10, the assumption of $\Delta T/T_0 = 1.0$ implies some fuel other than a hydrocarbon at the higher Mach numbers.

The thrust specific impulse is defined as

$$I = \frac{F}{w_f} \quad (E3)$$

From the conservation of heat and energy,

$$\frac{w_f}{w_a} = \frac{c_p \Delta T}{h} \quad (E4)$$

The weight of airflow is

$$w_a = \frac{g \rho_0 M A_0}{a} \quad (E5)$$

From these relations, the thrust specific impulse over the heating value of the fuel, or thrust per Btu per second, is

$$\frac{F}{Q} = \frac{I}{h} = \frac{\left[C_V \sqrt{\eta_e} \sqrt{1 + \frac{\Delta T}{t \left(1 + \frac{\gamma - 1}{2} M^2 \right)}} - 1 \right] Ma}{g c_p \Delta T} \quad (E6)$$

A value of $C_V \sqrt{\eta_e} = 0.95$ appears experimentally achievable at the lower Mach numbers. This value and a more conservative value of 0.90 were used in figure 10. For an airplane initially cruising at maximum lift-drag ratio, the lift-drag ratio for maneuvering at cruise altitude is, in terms of the cruise lift-drag ratio,

$$\left(\frac{L}{D} \right)_n = \frac{2n}{1 + n^2} \left(\frac{L}{D} \right)_c \quad (E7)$$

where $n = 1.0$ corresponds to steady level flight. The specific lift parameter for thrust equal to drag may be written from equations (E6) and (E7) as

$$\frac{L}{Q} = \frac{F}{Q} \frac{L}{D} = \frac{\left[\sqrt{\eta_e} C_V \sqrt{1 + \frac{\Delta T}{t \left(1 + \frac{\gamma - 1}{2} M^2 \right)}} - 1 \right] Ma \left[\left(\frac{L}{D} \right)_c 2n \right]}{c_p g \Delta T \left[\frac{1 + n^2}{1 + n^2} \right]} \quad (E8)$$

or

$$\frac{L}{Q} = \frac{\left[\sqrt{\eta_e} C_V \sqrt{1 + \frac{\Delta T}{t \left(1 + \frac{\gamma - 1}{2} M^2 \right)}} - 1 \right] t M (\gamma - 1) J \left[\left(\frac{L}{D} \right)_c 2n \right]}{\Delta T \left[\frac{1 + n^2}{1 + n^2} \right]} \quad (E9)$$

The wing lift coefficient for cruise at maximum lift-drag ratio is

$$C_L = \frac{2}{\sqrt{M^2 - 1} \left(L/D \right)_c} \quad (E10)$$

This may be compared with the lift coefficient for underwing heat addition given by equations (B30) and (B31). A cruise L/D of 5.0 or 6.0 is consistent with the present experimental results at high Mach numbers.

APPENDIX F

PERFORMANCE OF COMPOSITE SYSTEMS

This appendix considers simple wing and engine systems combining ramjet propulsion and underwing heat addition. Considered in this paragraph is the case of a wing designed for underwing heat addition with part of the thrust required to overcome the wing drag provided by a ramjet. The previous derivations and results can be reinterpreted to cover this case. The C_D in the parameter $\beta C_D / (\tau/c)^2$ is the thrust coefficient developed by underwing heat addition, over and above the thrust required to overcome the wing pressure drag. For an isolated wing, the only remaining drag force is the friction drag. Hence, the thrust to be provided by a ramjet is

$$C_{F,r} = 2C_{fr} - \left[\frac{\beta C_D}{(\tau/c)^2} \right] \frac{(\tau/c)^2}{\beta} \quad (F1)$$

The L/Q for the composite case may be written

$$\frac{L}{Q} = \frac{\frac{L}{C_{F,r} q c}}{\frac{1}{\left(\frac{I}{h}\right)_r} + \frac{L_u}{\left(\frac{L}{Q}\right)_u}} \quad (F2)$$

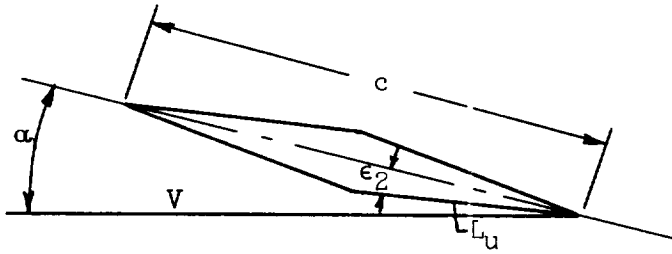
($q = \frac{\gamma}{2} p M^2$ in this appendix), or in coefficient form

$$\frac{L}{Q} = \frac{\frac{C_{L,u}}{C_{F,r}}}{\frac{1}{\left(\frac{I}{h}\right)_r} + \frac{C_{L,u}}{\left(\frac{L}{Q}\right)_u}} \quad (F3)$$

The lift coefficient is that for underwing heat addition and may be determined from the parameter $C_L / (\tau/c)$ of figure 3(d). The L/Q may be determined from figures 3(a) and (b) for the linearized theory. The I/h for the ramjet may be calculated from equation (E6). The terms in the denominator of equation (F3) are respectively proportional to the Btu input to the ramjet and the underwing heating. The fraction of the total heat input to the ramjet can thus be found.

This paragraph considers the case of the conventional ramjet plus wing with some heat addition. The calculation is made assuming a constant lift coefficient having the value for maximum lift-drag ratio with no heat addition. From linearized theory the optimum wing shape for a

given thickness ratio is a double wedge with half the thickness on each side of a straight line joining the leading and trailing edges. The following sketch shows the type of airfoil:



The wing angle of attack is related to the heat addition under the wing by

$$\frac{Q_u}{qc} = \frac{C_{L,\text{opt}} - \left(\frac{dC_L}{d\alpha}\right)\alpha}{(L/Q)_u} \quad (\text{F4})$$

The drag to be overcome by ramjet thrust is

$$C_{F,r} = C_D = 2C_{fr} + \frac{4(\tau/c)^2}{\beta} + \left(\frac{dC_L}{d\alpha}\right)\alpha^2 + \left(\frac{L}{Q}\right)_{l,\alpha=0} \frac{Q_u}{qc} (\alpha - \epsilon_2) \quad (\text{F5})$$

The heat input to the ramjet is

$$\frac{Q_r}{qc} = \frac{C_{F,r}}{\left(\frac{I}{h}\right)_r} \quad (\text{F6})$$

The over-all L/Q is then

$$\frac{L}{Q} = \frac{C_{L,\text{opt}}}{\frac{Q_u}{qc} + \frac{Q_r}{qc}} \quad (\text{F7})$$

The fraction of the total heat input consumed in the ramjet may be calculated from equations (F4) and (F6). For a two-dimensional unswept wing of double-wedge profile, the linearized theory gives the following relations required in the preceding equations:

$$\frac{1}{\left(\frac{C_{D,L}}{C_L^2}\right)} = \frac{dC_L}{d\alpha} = \frac{4}{\beta} \quad (\text{F8})$$

$$c_{D,0} = 2c_{fr} + \frac{4(\tau/c)^2}{\beta} \quad (F9)$$

and

$$c_{L,opt} = \sqrt{\frac{c_{D,0}}{(c_{D,i}/c_L^2)}} \quad (F10)$$

In the example in the text, it is assumed that $M = 8$, $\tau/c = 0.03$, and $c_{fr} = 0.001$.

REFERENCES

1. Pinkel, I. Irving, and Serafini, John S.: Graphical Method for Obtaining Flow Field in Two-Dimensional Supersonic Stream to Which Heat Is Added. NACA TN 2206, 1950.
2. Pinkel, I. Irving, Serafini, John S., and Gregg, John L.: Pressure Distribution and Aerodynamic Coefficients Associated with Heat Addition to Supersonic Air Stream Adjacent to Two-Dimensional Supersonic Wing. NACA RM E51K26, 1952.
3. Mager, Artur: Supersonic Airfoil Performance with Small Heat Addition. Preprint 768, Inst. Aero. Sci., 1958.
4. Gazley, Carl, Jr.: Linearized Solution for Heat Addition at the Surface of a Supersonic Airfoil. RM-1892, The RAND Corp., Nov. 21, 1956. (AD 133025.)
5. Lomax, Harvard: Two Dimensional, Supersonic, Linearized Flow with Heat Addition. NASA MEMO 1-10-59A, 1959.
6. Fletcher, Edward A., Dorsch, Robert G., and Gerstein, Melvin: Combustion of Aluminum Borohydride in a Supersonic Wind Tunnel. NACA RM E55D07a, 1955.
7. Dorsch, Robert G., Serafini, John S., and Fletcher, Edward A.: A Preliminary Investigation of Static-Pressure Changes Associated with Combustion of Aluminum Borohydride in a Supersonic Wind Tunnel. NACA RM E55F07, 1955.
8. Serafini, John S., Dorsch, Robert G., and Fletcher, Edward A.: Exploratory Investigation of Static- and Base-Pressure Increases Resulting from Combustion of Aluminum Borohydride Adjacent to Body of Revolution in Supersonic Wind Tunnel. NACA RM E57E15, 1957.
9. Dorsch, Robert G., Serafini, John S., and Fletcher, Edward A.: Exploratory Investigation of Aerodynamic Effects of External Combustion of Aluminum Borohydride in Airstream Adjacent to Flat Plate in Mach 2.46 Tunnel. NACA RM E57E16, 1957.
10. Evans, Philip J., Jr.: Analytical Investigation of Ram-Jet-Engine Performance in Flight Mach Number Range from 3 to 7. NACA RM E51H02, 1951.

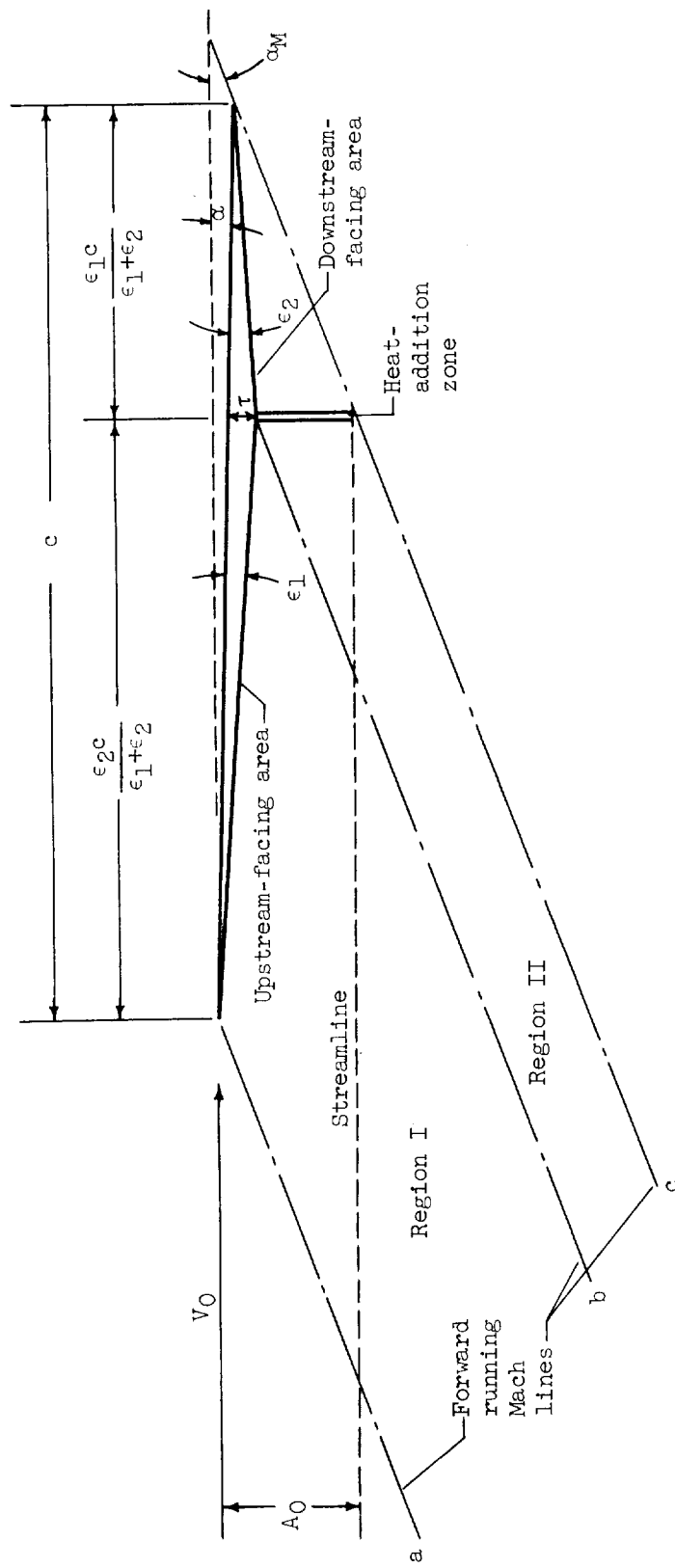


Figure 1. - General wing and heat-addition geometry.

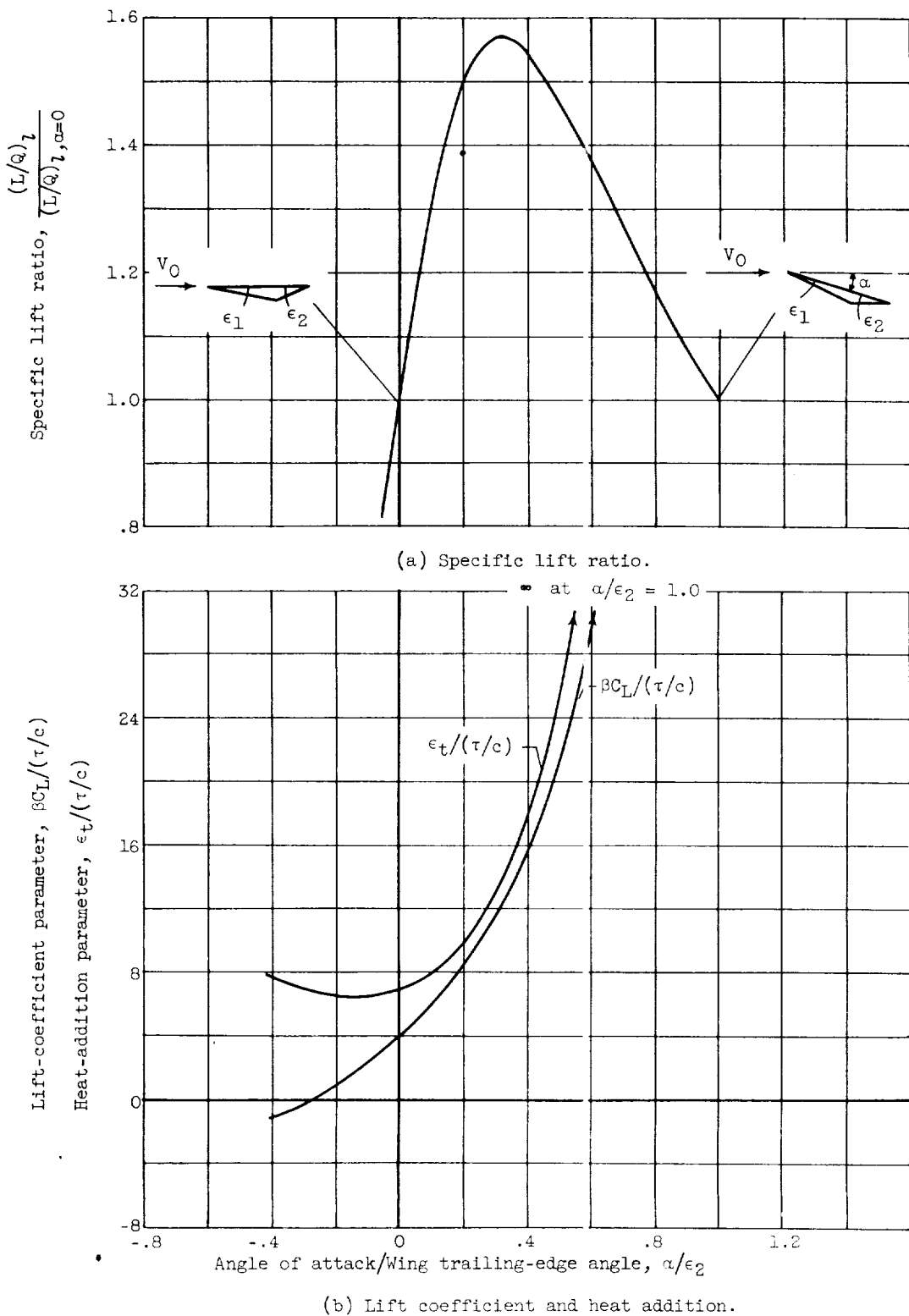


Figure 2. - Typical effect of angle of attack on performance of wing with heat addition. Linearized theory; $\beta C_D / (\tau/c)^2 = 4.0$; $\epsilon_1/\epsilon_2 = 0.4$.

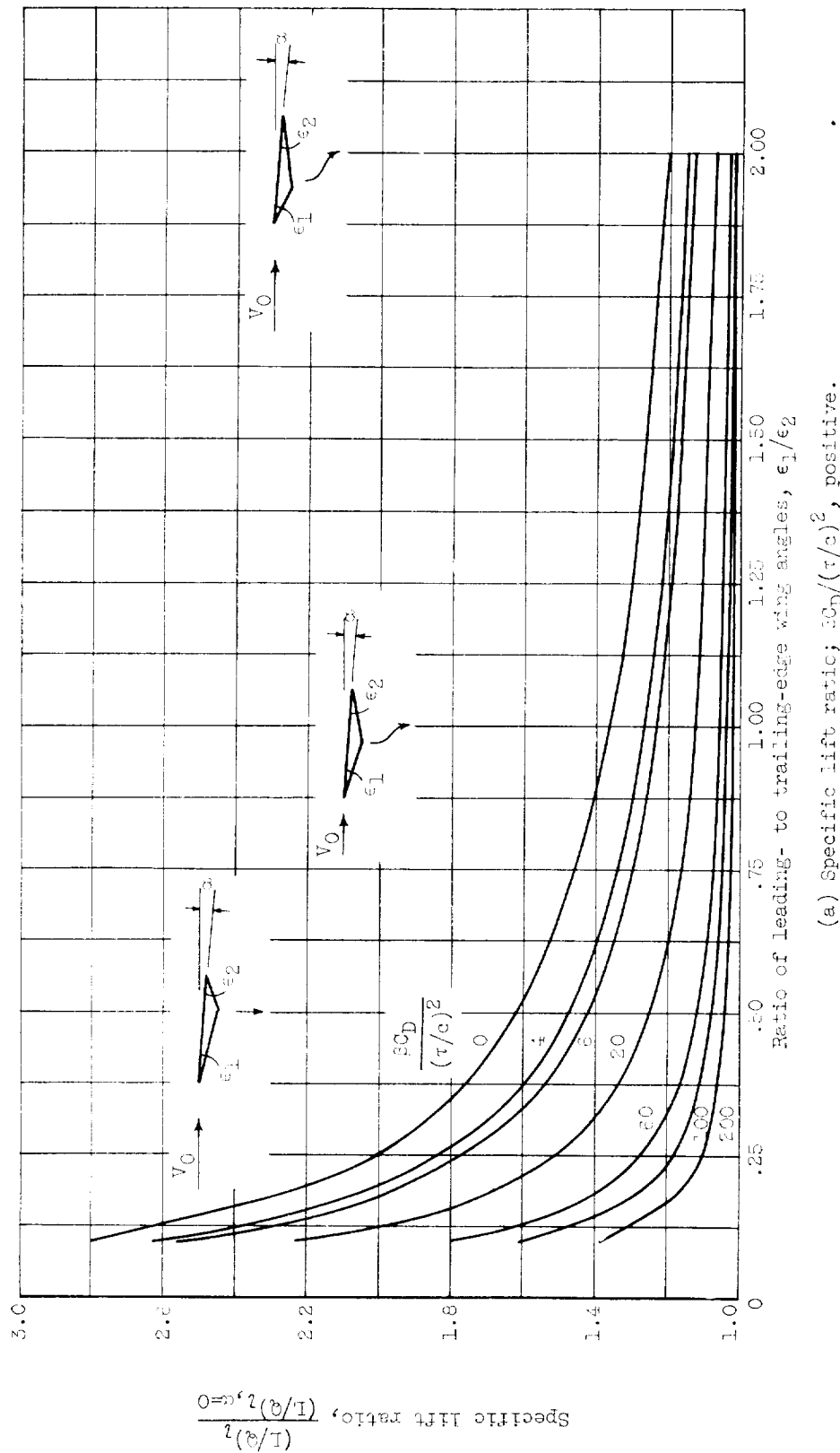
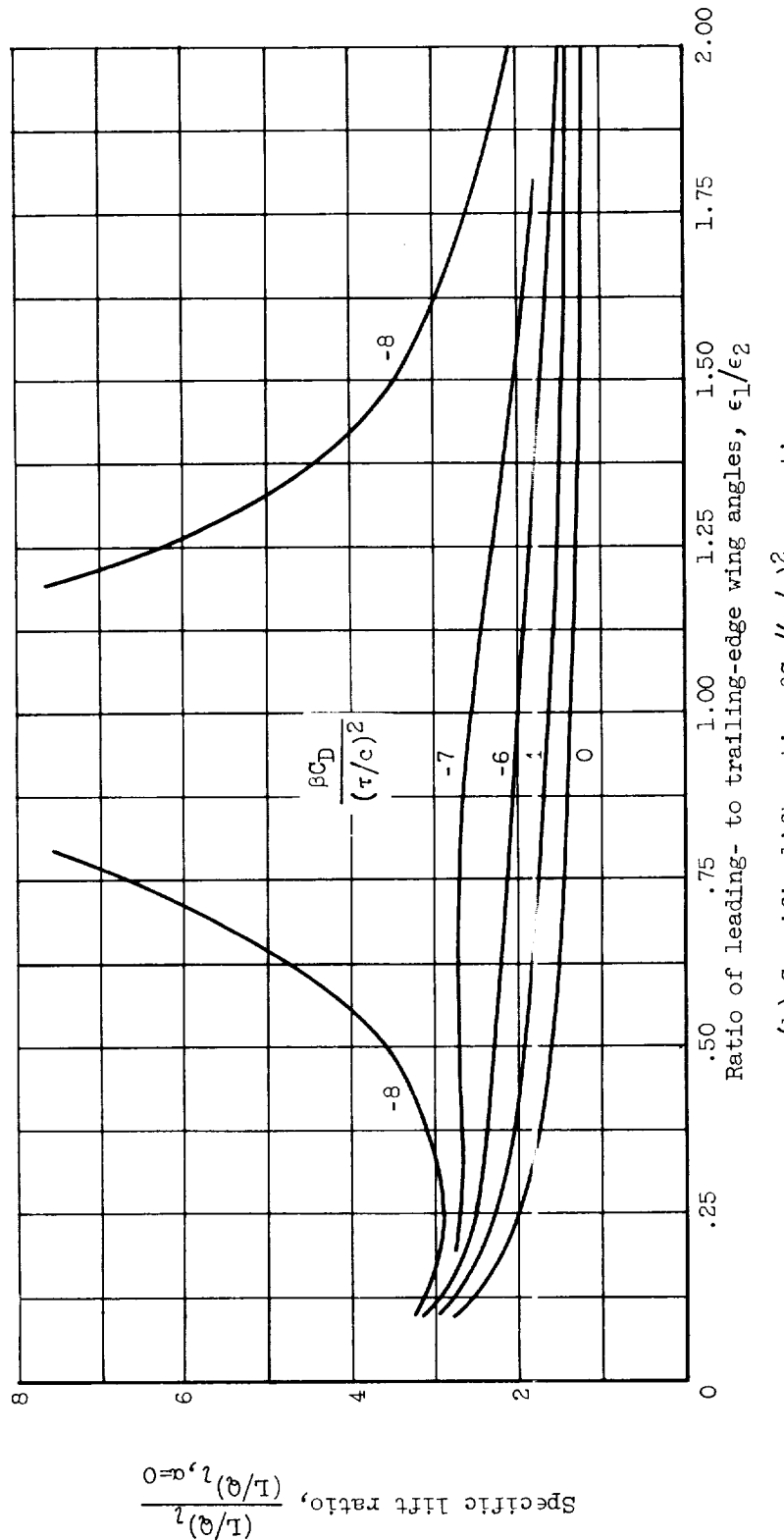
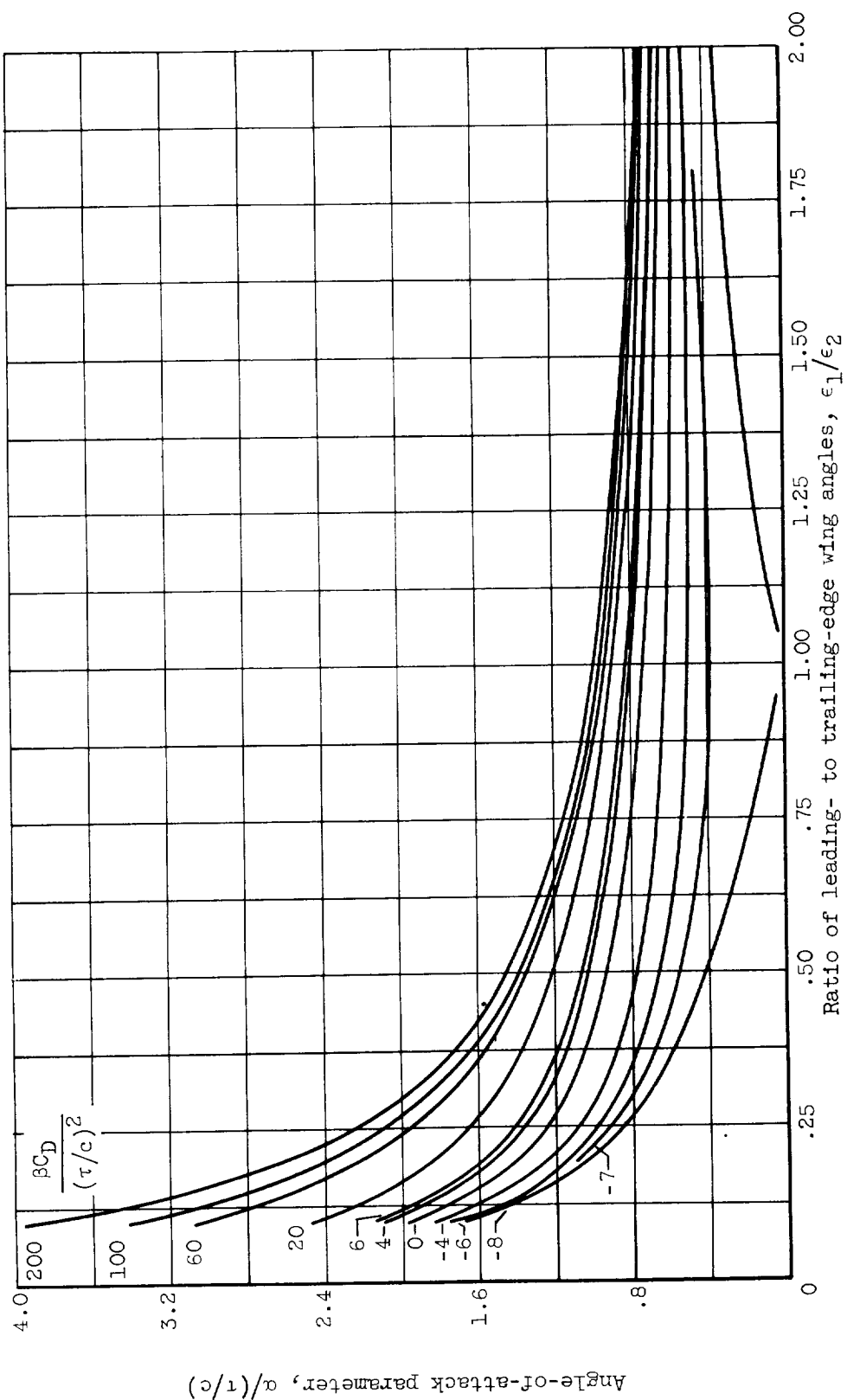


Figure 3. - Effect of maximum-thickness location on performance of wing at optimum angle of attack with heat addition. Linearized theory.
 (a) Specific lift ratio; $C_D/(\tau/c)^2$, positive.



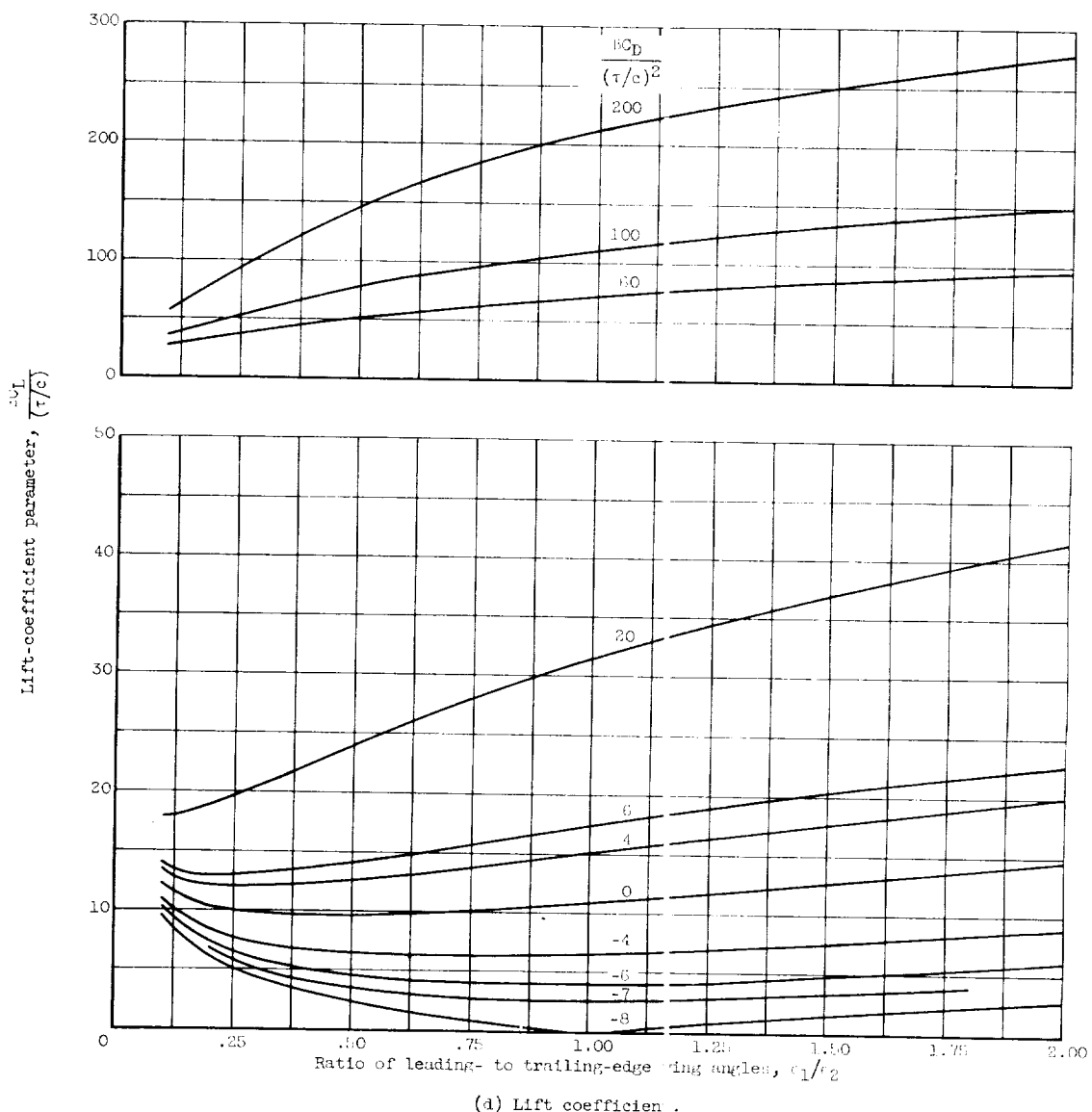
(b) Specific lift ratio; $\beta C_D / (\tau/c)^2$, negative.

Figure 3. - Continued. Effect of maximum-thickness location on performance of wing at optimum angle of attack with heat addition. Linearized theory.



(c) Optimum angle of attack.

Figure 3. - Continued. Effect of maximum-thickness location on performance of wing at optimum angle of attack with heat addition. Linearized theory.



(d) Lift coefficient .

Figure 3. - Continued. Effect of maximum-thickness location on performance of wing at optimum angle of attack with heat addition. Linearized theory.

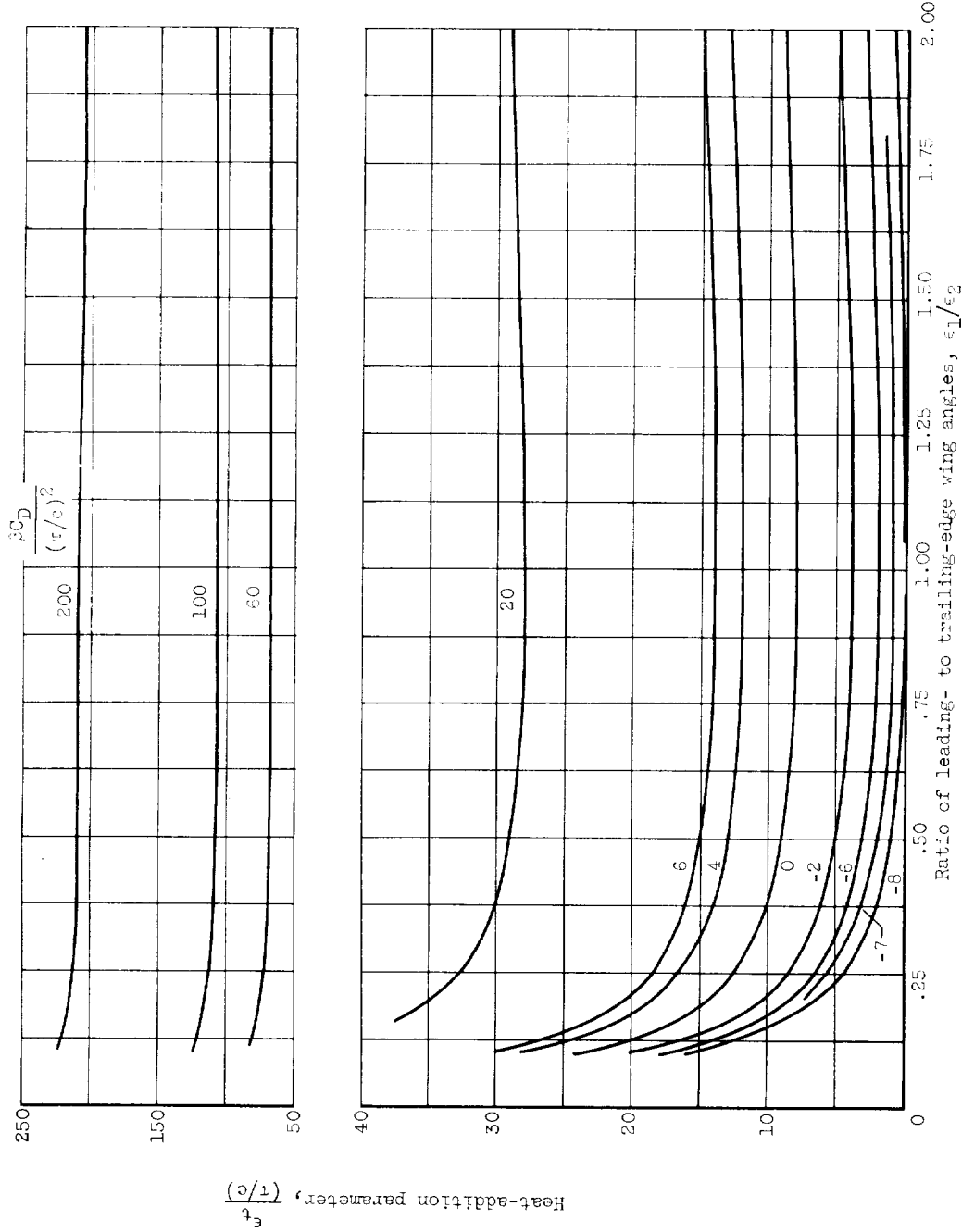


Figure 3. - Concluded. Effect of maximum-thickness location on performance of wing at optimum angle of attack with heat addition. Linearized theory.
(e) Heat addition.

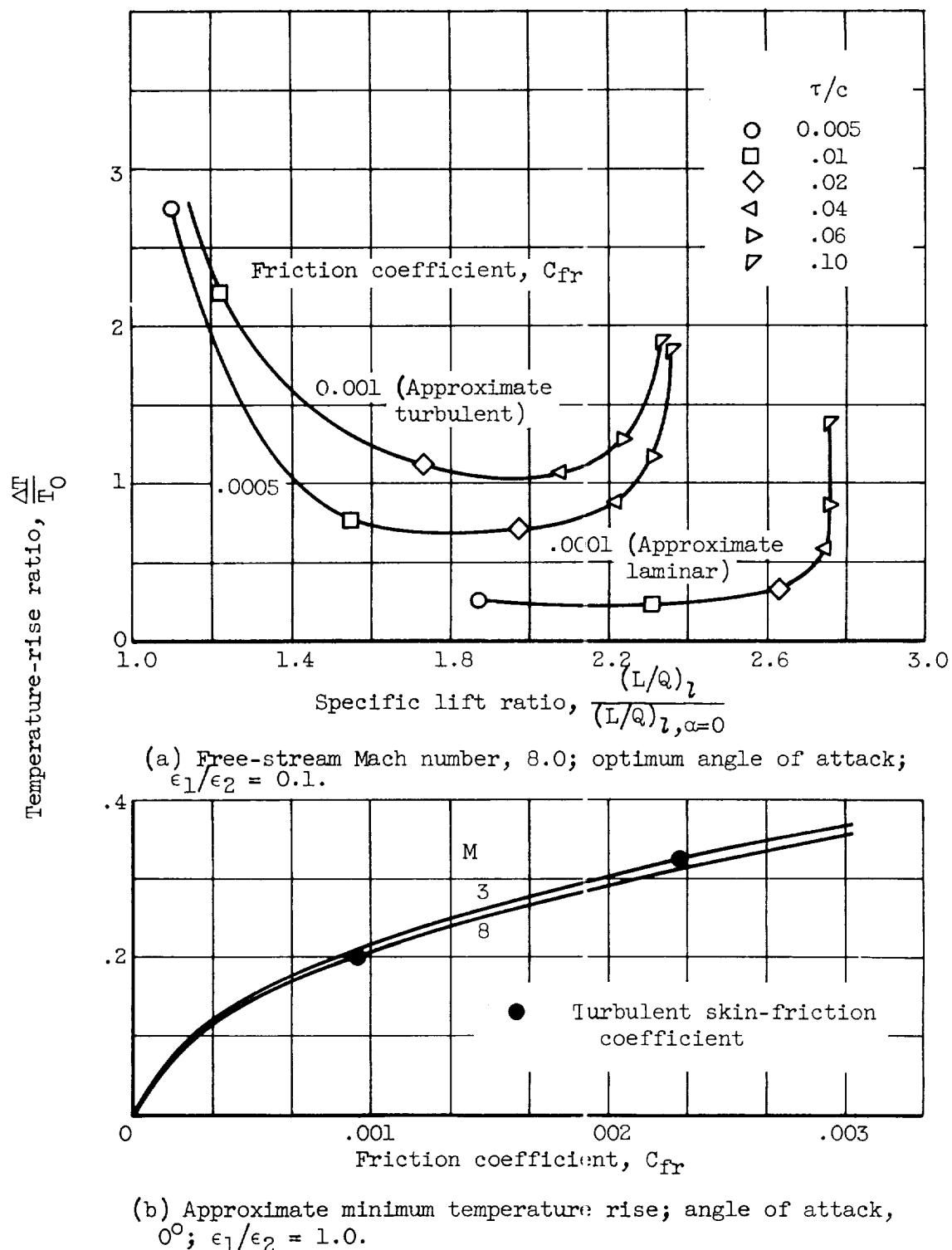


Figure 4. - Temperature-rise ratios. Linearized theory.

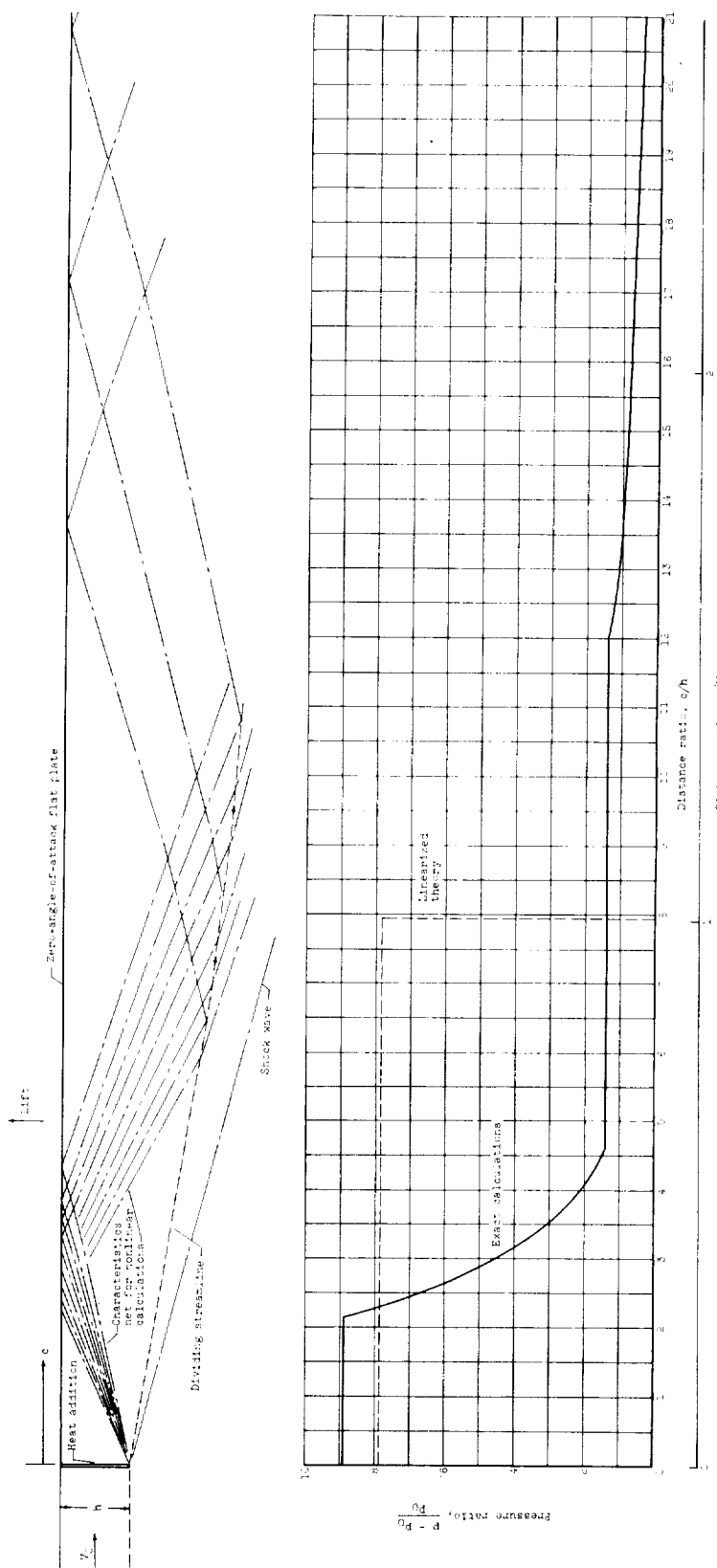


Figure 5. - Typical pressure distribution on zero-angle-of-attack flat plate with heat addition as determined by nonlinearized calculations and linearized theory. Free-stream Mach number, 8.0; temperature-rise ratio, 0.4; free-stream static temperature, 392° R.

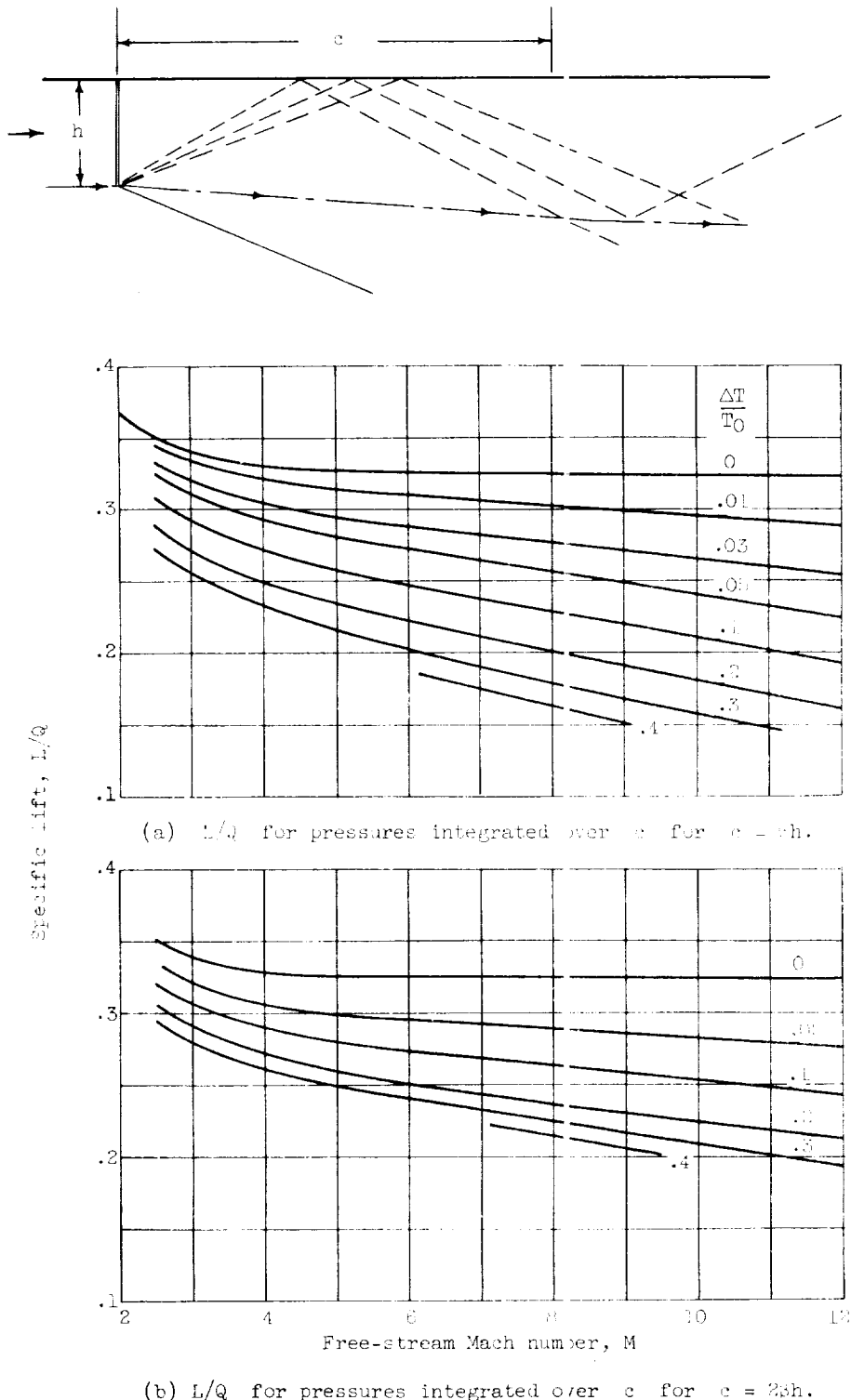


Figure 6. - Nonlinearized calculation of specific lift for flat plate at zero angle of attack. Free-stream static temperature, 392° R.

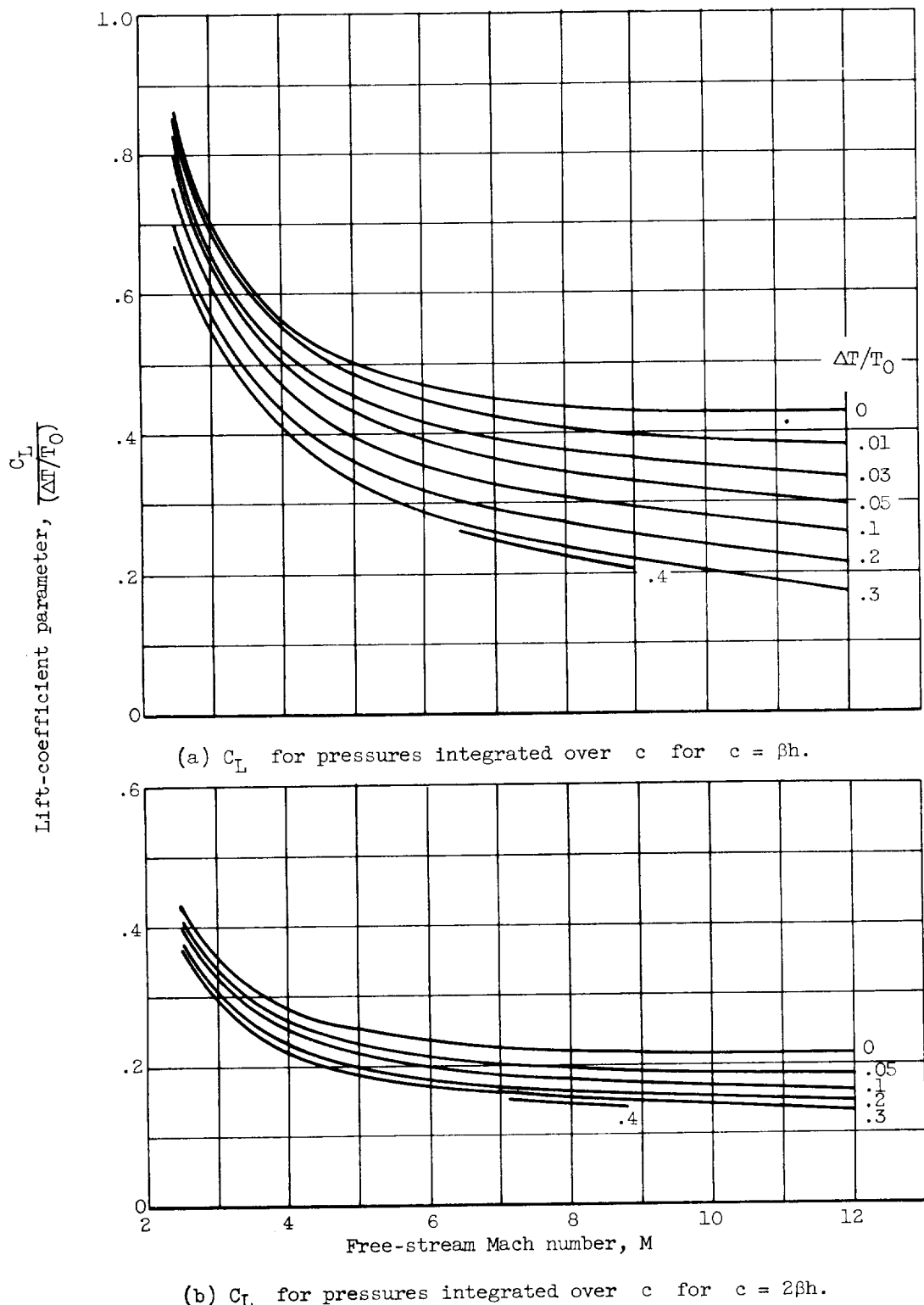


Figure 7. - Nonlinearized calculation of lift coefficient for flat plate at zero angle of attack. Free-stream static temperature, 392° R.

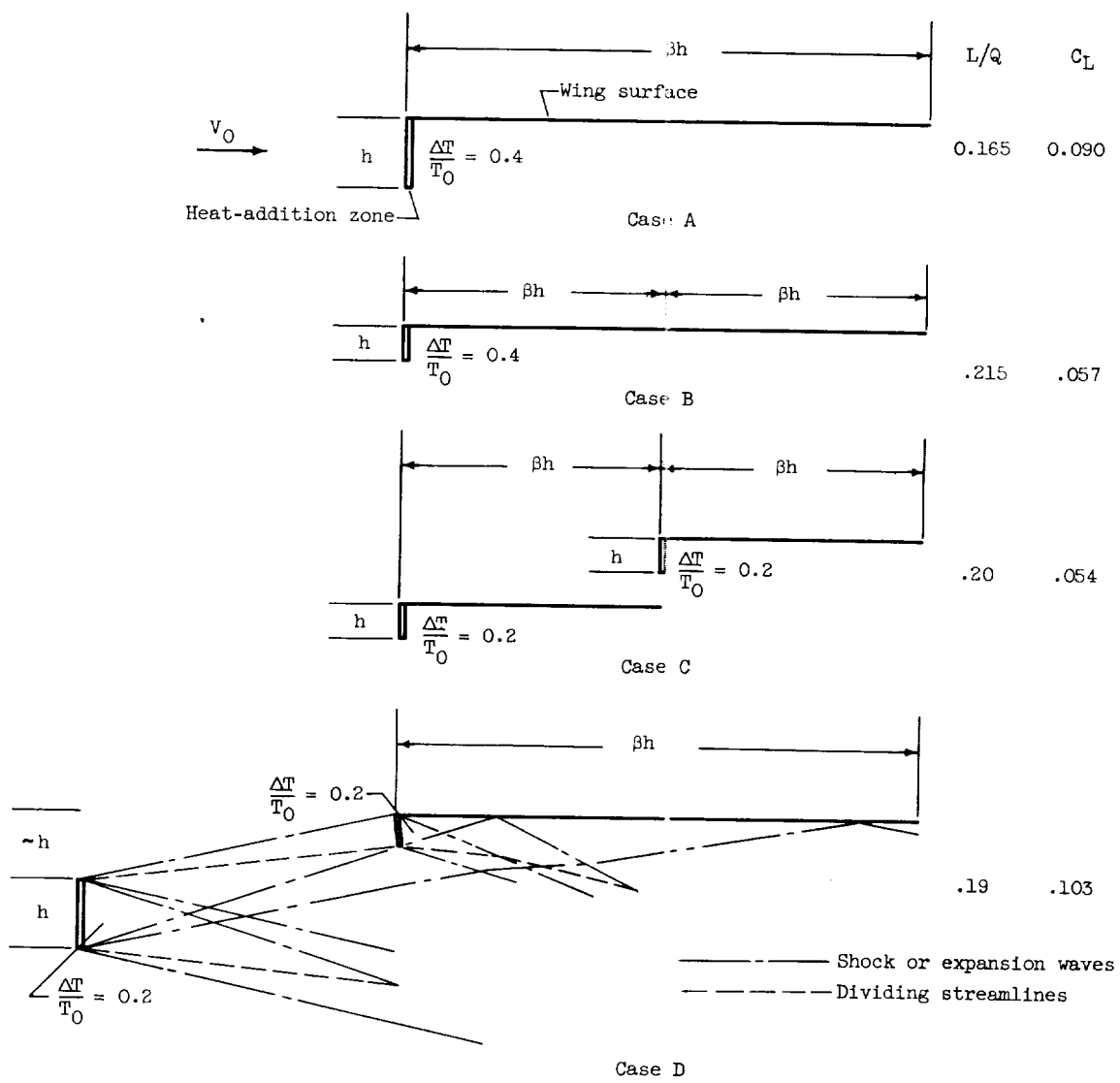


Figure 8. - Effect of heat distribution. Free-stream Mach number, 8.0.

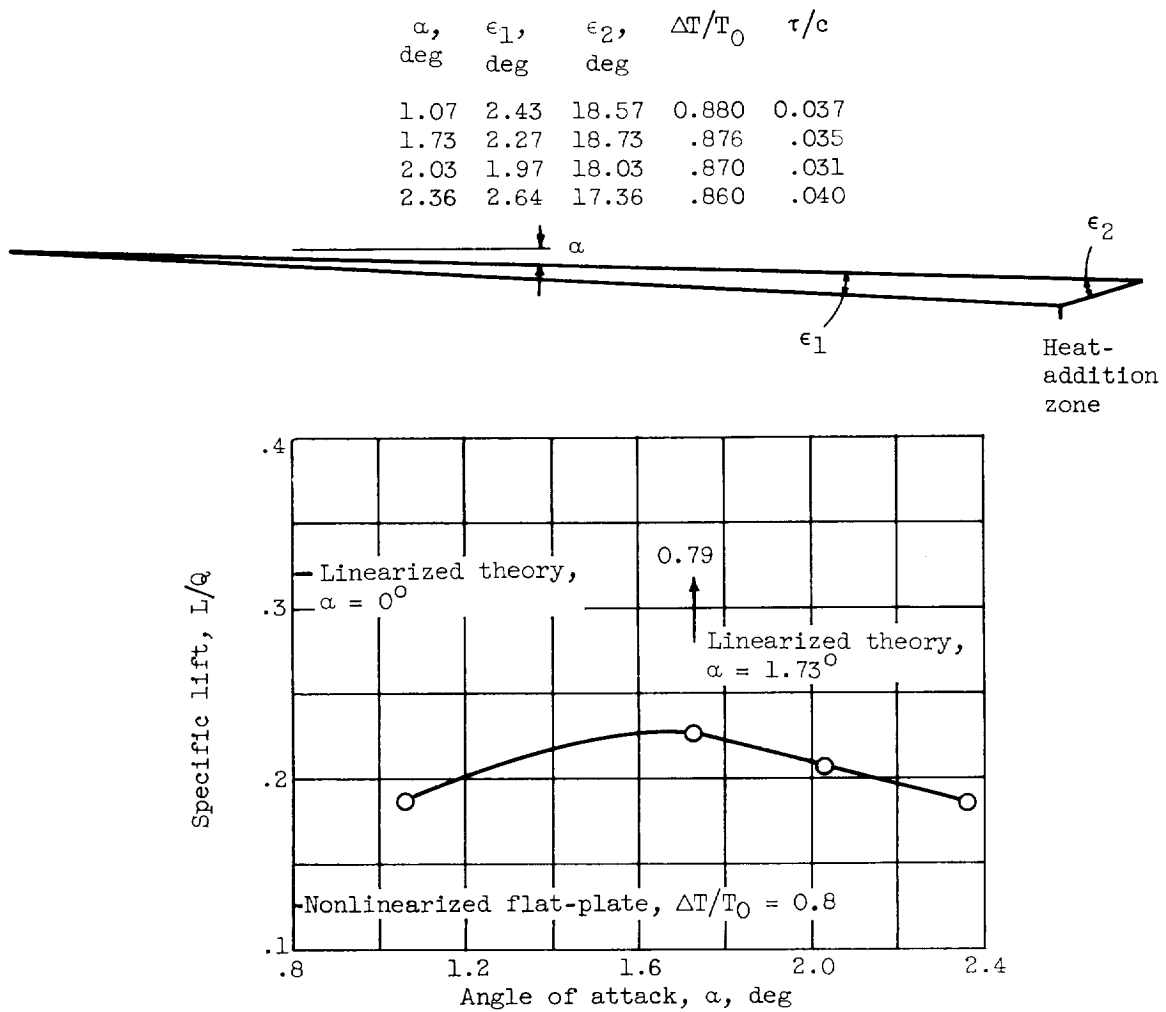


Figure 9. - Nonlinearized calculation of specific lift for several wings. Friction coefficient, 0.00095; free-stream static temperature, 392° R.

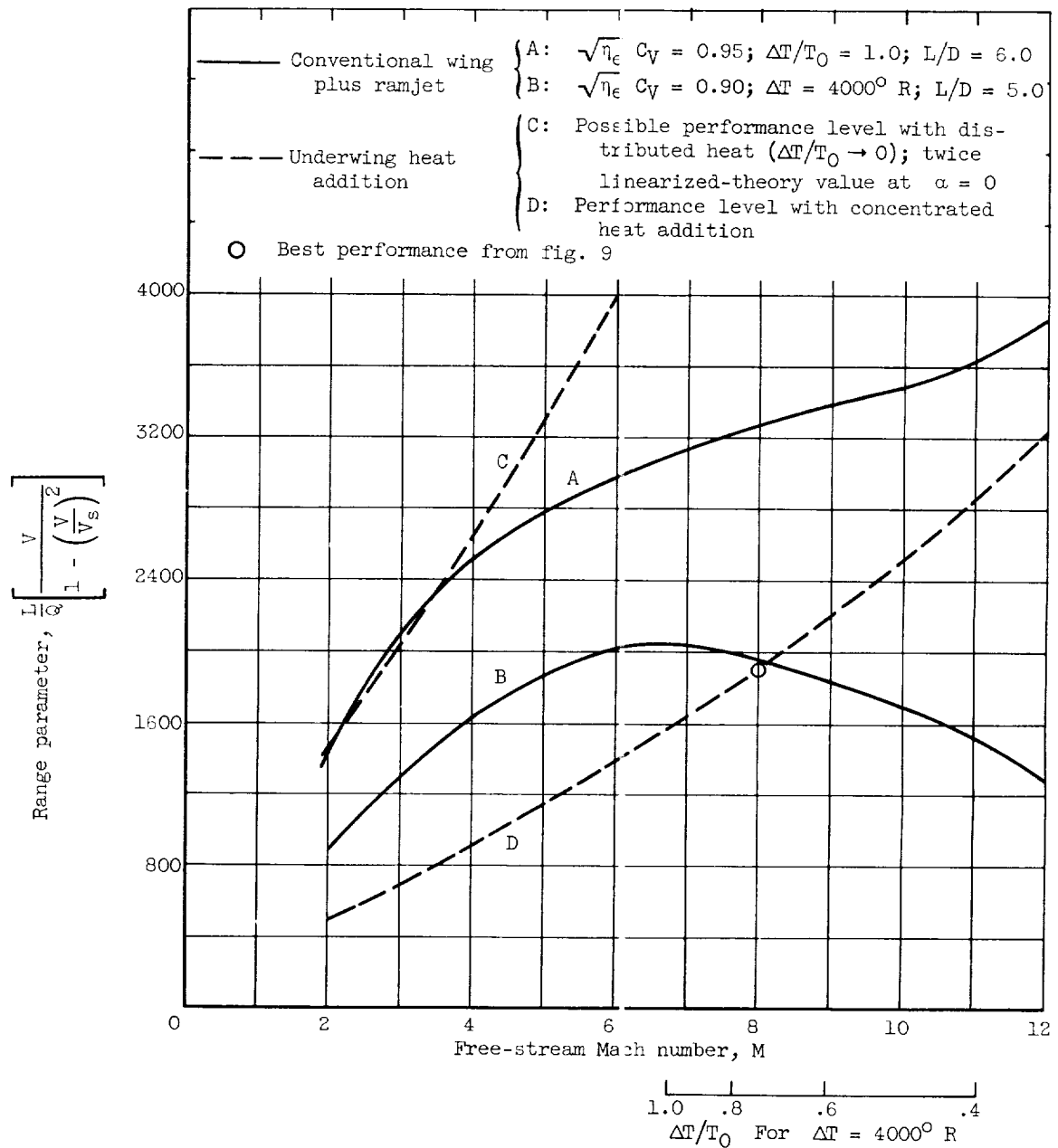
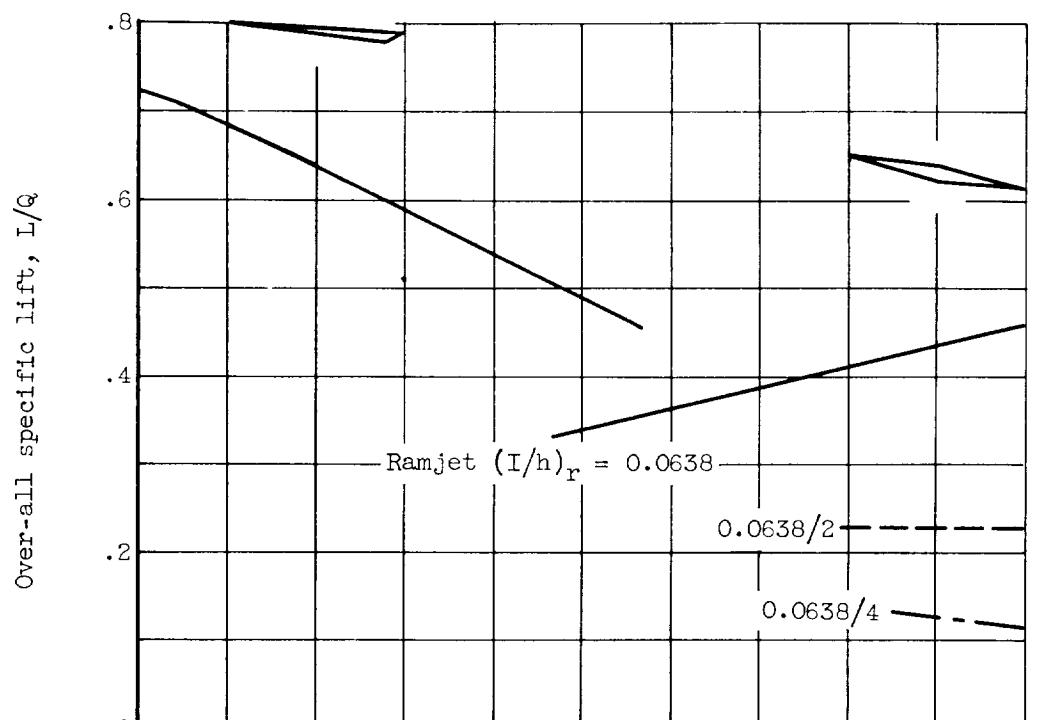
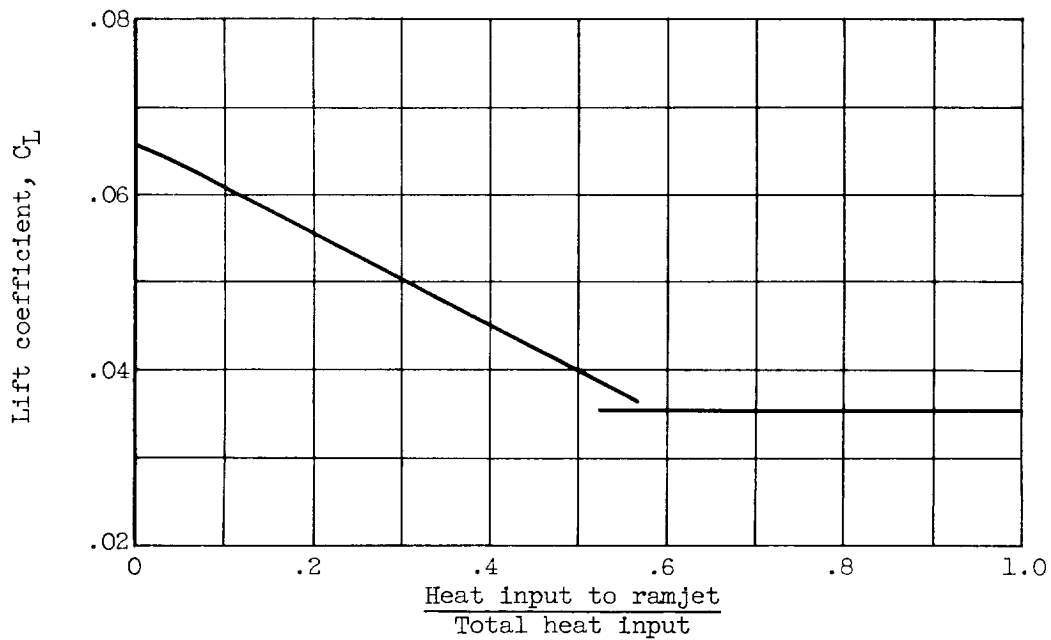


Figure 10. - Comparison of cruise efficiency of underwing heat addition and conventional wing plus ramjet. Free-stream static temperature, $392^\circ R$.

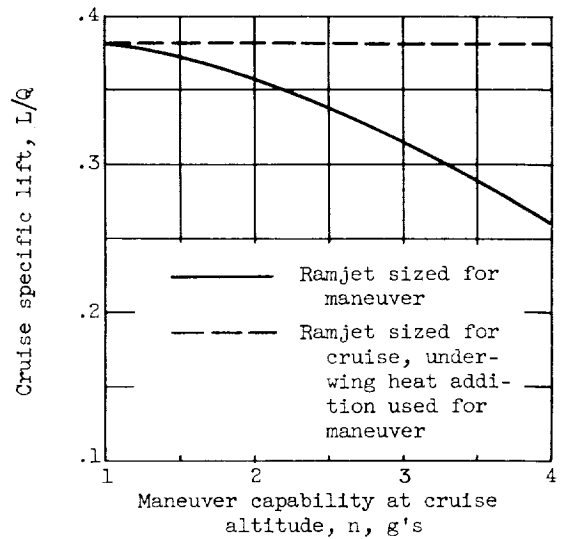


(a) Specific lift.

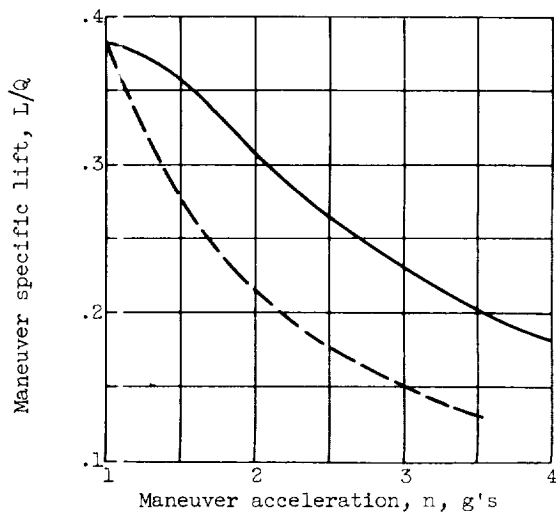


(b) Lift coefficient.

Figure 11. - Cruise performance when propulsion is by combined ramjet and underwing heat addition. Free-stream Mach number, 8.0; free-stream static temperature, 392° R.

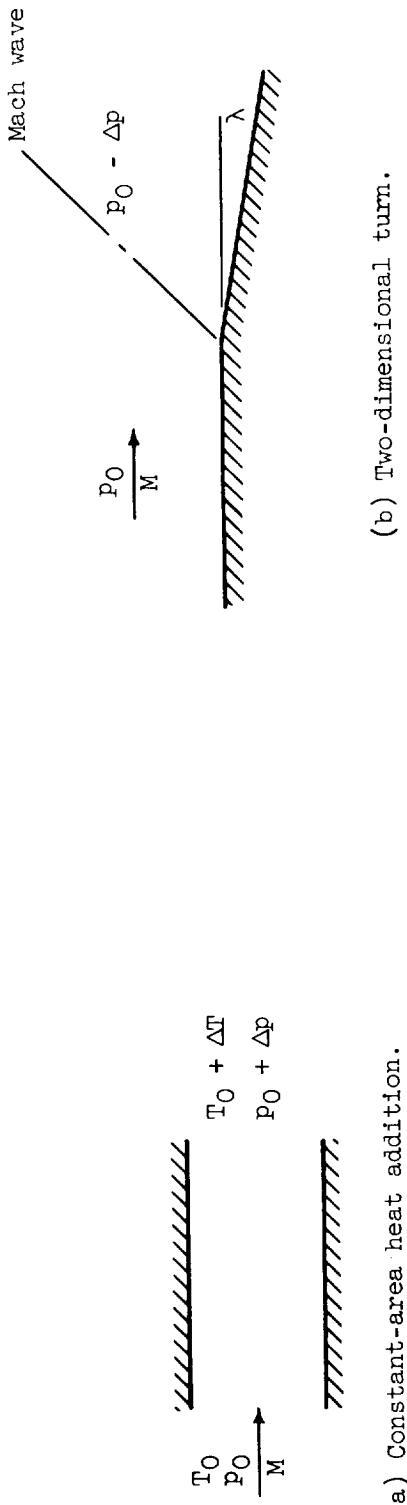


(a) Cruise performance.



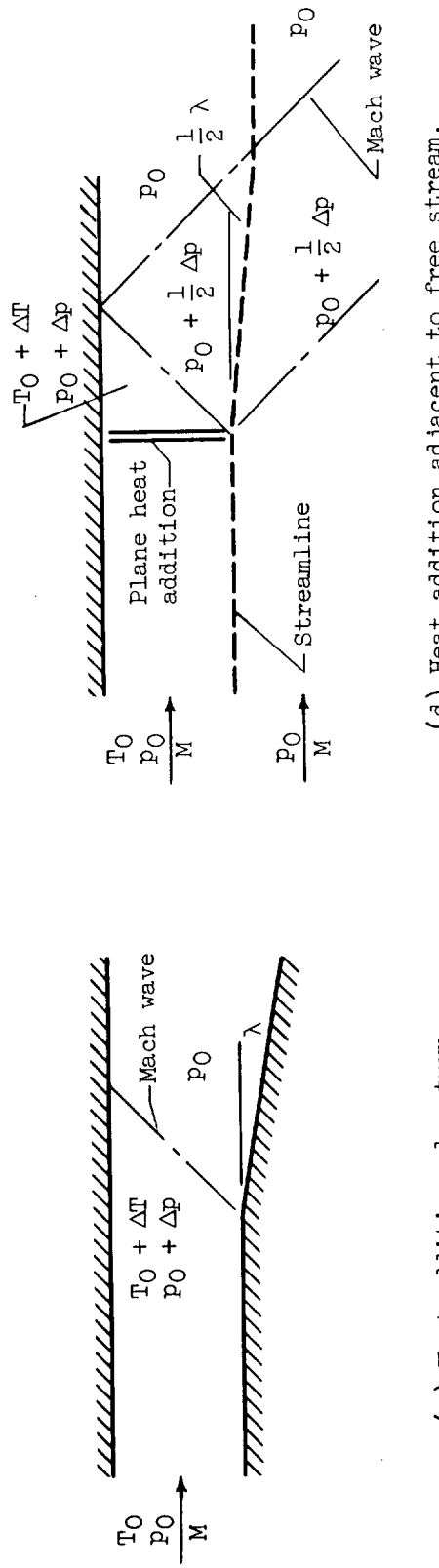
(b) Maneuver performance.

Figure 12. - Cruise and maneuver performance when maneuver capability is required.
Propulsion by combined ramjet and underwing heat addition. Free-stream Mach number, 8.0; free-stream static temperature, 392° R.



(a) Constant-area heat addition.

(b) Two-dimensional turn.



(b) Two-dimensional turn.

(c) Heat addition plus turn.

(d) Heat addition adjacent to free stream.

